Chemistry—A European Journal

Full Paper
doi.org/10.1002/chem.202003170

**Chemistry
Europe**
European Chemical
Societies Publishing

▌ Organometallic Chemistry

Enantiomerically Pure Constrained Geometry Complexes of the Rare-Earth Metals Featuring a Dianionic N-Donor Functionalised Pentadienyl Ligand: Synthesis and Characterisation

Katharina Münster, Ann Christin Fecker, Jan Raeder, Matthias Freytag, Peter G. Jones, and Marc D. Walter*[a]

Abstract: We report the preparation of enantiomerically pure constrained geometry complexes (*cgc*) of the rare-earth metals bearing a pentadienyl moiety (pdl) derived from the natural product (1*R*)-(−)-myrtenal. The potassium salt **1**, [Kpdl*], was treated with ClSiMe₂NH*t*Bu, and the resulting pentadiene **2** was deprotonated with the *Schlosser*-type base KO*t*Pen/*n*BuLi (*t*Pen = CMe₂(CH₂Me)) to yield the dipotassium salt [K₂(pdl*SiMe₂N*t*Bu)] (**3**). However, **3** rearranges in THF solution to its isomer **3′** by a 1,3-H shift, which elongates the bridge between the pdl and SiMe₂N*t*Bu moieties by one CH₂ unit. This is crucial for the successful formation of various monomeric *C*₁- or dimeric *C*₂-symmetric rare-earth *cgc* complexes with additional halide, tetraborohydride, amido and alkyl functionalities. All compounds have been extensively characterised by solid-state X-ray diffraction analysis, solution NMR spectroscopy and elemental analyses.

Introduction

Since the first report on "constrained geometry complexes" (*cgc*s) in 1990 by Bercaw and co-workers,[1] this area has attracted significant academic and industrial interest because of its relevance in stereocontrolled catalysis and catalyst design in general. Like *ansa*-metallocenes, *cgc*s offer a wide range of structural diversity, since their three main components, viz. the π-donor, bridge and σ-donor functionalities (Figure 1), can all be varied individually, which influences not only the Lewis acidity but also the steric accessibility (via the bite angle) of
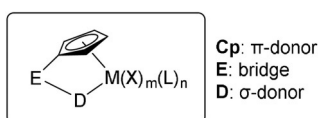

Figure 1. General formula of a constrained geometry complex (*cgc*).[2a]

[a] *K. Münster, Dr. A. C. Fecker, J. Raeder, Dr. M. Freytag, Prof. Dr. P. G. Jones, Prof. Dr. M. D. Walter*
Institut für Anorganische und Analytische Chemie
Technische Universität Braunschweig
Hagenring 30, 38106 Braunschweig (Germany)
E-mail: mwalter@tu-bs.de

📄 *Supporting information and the ORCID identification number(s) for the author(s) of this article can be found under:*
https://doi.org/10.1002/chem.202003170.

the central metal atom.[2] Whereas Bercaw and co-workers synthesised various scandium compounds with a dimethylsilyl-*tert*-butyl-amine functionalised tetramethyl-cyclopentadienyl moiety,[1,3] Okuda and co-workers developed the related titanium and iron complexes [(Me₃C(C₅H₃))SiMe₂N(CMe₃)MX₂] (M = Ti, X = Cl; M = Fe, X = CO).[4]

Hence, silylamido-functionalised cyclopentadienyl (Cp) ligands are well-known for group 3 and 4 transition metals, whereas the functionalisation of pentadienyls (pdl) has so far only been reported for neutral *N*-donor units. However, an "open" pdl system should significantly alter the reactivity of the metal compound because of its better π-donor and δ-acceptor properties. Furthermore, the ability of the pdl ligand to adopt different coordination modes enhances the flexibility of the coordination sphere at the metal atom (Figure 2).[5] For example, Layfield and co-workers presented lithiated pdl complexes bearing neutral silylamine linkers,[6] as well as donor-substituted dysprosium pdl compounds.[7] Meanwhile, our group realised the synthesis of an enantiomerically pure pdl system with a neutral N-donor functionality. However, the additional neutral N-donor moiety in the chiral pdl systems does not coordinate to the metal atom, thus preventing *cgc* formation in these cases (Figure 2).[8] Based on these results, we now present the synthesis and structural characterisation of the first pdl system with an anionic donor function, yielding *cgc*s with the rare-earth metals by η⁵ (or η³) and κ-N coordination. This introduces a new structural motif in pentadienyl chemistry, and might also offer promising applications in (enantioselective) catalysis.[9]

Chemistry–A European Journal

Full Paper
doi.org/10.1002/chem.202003170

Chemistry Europe
European Chemical
Societies Publishing

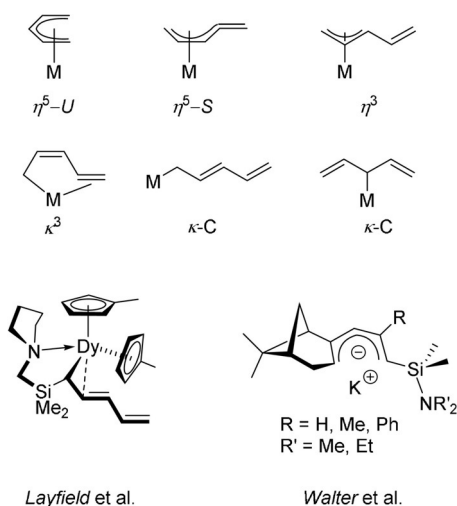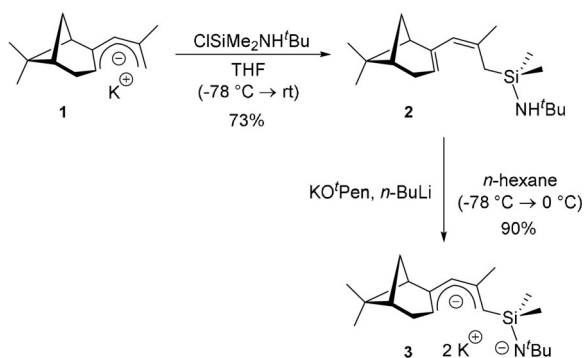**Figure 2.** Various coordination modes of the pdl ligand and examples of si-lylamine-functionalised pentadienyls.[5,7,8]

Figure 3. ^{1}H NMR spectrum (500 MHz, [D$_8$]THF) for the ligand rearrangement reaction at 55 °C.

Results and Discussion

Ligand synthesis

Based on our previous reports on myrtenal-derived pdl ligands (pdl*),[8,10] the enantiomerically pure potassium salt **1**, [Kpdl*], was reacted with ClSiMe$_2$NHtBu. Deprotonation of the resulting pentadiene **2** employing the *Schlosser*-type base KO^{t}Pen/nBuLi (^{t}Pen = CMe$_2$(CH$_2$Me)) affords the exceedingly moisture- and air-sensitive dipotassium salt [K$_2$(pdl*SiMe$_2$NtBu)] (**3**) in enantiomerically pure form as a yellow, pyrophoric solid (Scheme 1). Attention to detail is crucial; and it is essential to perform the reaction and work-up procedure below 0 °C to prevent degradation of the desired product. However, this can then be stored and handled at ambient temperature.

Scheme 1. Synthesis of silylamidopentadiene **2** and metalation to [K$_2$(pdl*SiMe$_2$NtBu)] (**3**).

Ligand rearrangement reaction

Dissolved in THF, the dianionic ligand **3** undergoes a 1,3-H shift to its isomer **3′**, exhibiting an elongated silylamido bridge (Figure 3). Both compounds were fully characterised by NMR spectroscopy and all resonances were assigned by 2D NMR spectra (see Supporting Information). This conversion was
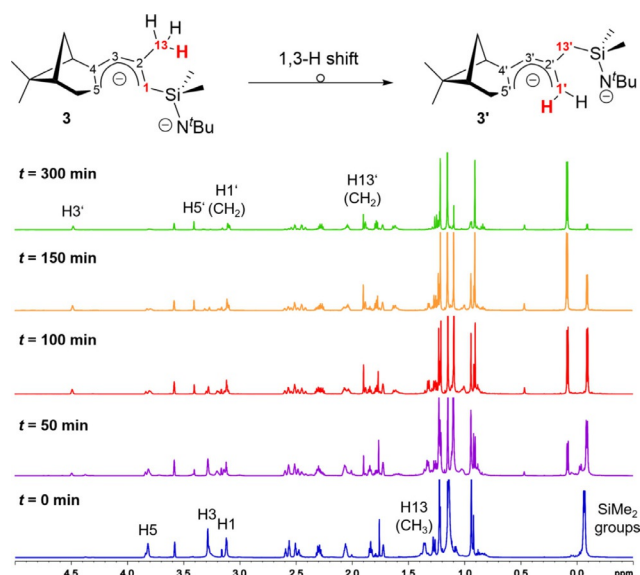
monitored by ^{1}H NMR in [D$_8$]THF solution at 55 °C, as shown in Figure 3. The progress can conveniently be followed by the downfield shift of the two respective singlets for the diastereotopic dimethylsilyl groups in each compound (**3**: $\delta = -0.10$, -0.08 ppm; **3′**: $\delta = 0.06$, 0.08 ppm) and the transformation of the methyl group in 4-position of the pdl (C13) to a bridging methylene group (C13′). In addition, the pdl proton at the 3-position (H3) undergoes a significant downfield shift from $\delta = 3.30$ ppm to $\delta = 4.52$–4.47 ppm, indicating a more localised negative charge at this position than in the starting material, where the negative charge is mainly situated at C5.

Synthesis of constrained geometry complexes

The dianionic ligand **3** can successfully be employed for the preparation of various rare-earth metal(III) complexes with halide, amido, tetraborohydride, triflate and alkyl substituents, as shown in Figure 4. These highly air- and moisture-sensitive compounds are difficult to crystallise; and attention to detail during synthesis, work-up and crystallisation is crucial. Therefore, we isolated them in pure form, but relatively low yields (20–40 %). All *cgc* products contain the ligand in its isomeric form **3′**. Clearly, the ligand rearrangement from **3** to **3′** is essential to realise the *cgc* architecture at the metal atom. Herein, the π-donor unit is represented by the pdl ligand, while the *tert*-butylamide function serves as the σ-donor unit. The compounds were extensively characterised employing elemental analysis, melting point determination, solid-state single-crystal X-ray diffraction analysis and solution NMR spectroscopic studies; X-ray and NMR results will be discussed in more detail in each section. All compounds are thermally stable up to at least 120 °C, and most of them melt reversibly without decomposition (for details see Experimental Section).
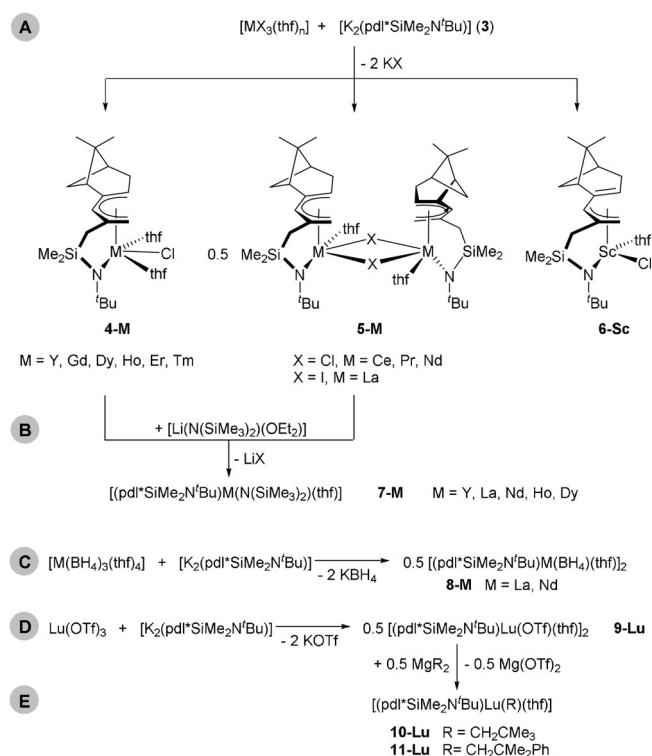
Chemistry–A European Journal

Full Paper
doi.org/10.1002/chem.202003170

Chemistry Europe
European Chemical
Societies Publishing

Figure 4. Use of the dianionic pdl ligand **3** to synthesise constrained geometry complexes with various substituents.

Synthesis of rare-earth metal halide complexes

The appropriate rare-earth metal halide reacts with a THF solution of **3** under an N_2 atmosphere at ambient temperature. After work-up and crystallisation, the diamagnetic (Ln = Y, Sc, La) and paramagnetic (Ln = Ce, Pr, Nd, Gd, Dy, Ho, Er, Tm)

metal complexes can be isolated (see Supporting Information for details, and Figure 4 A).

Solid-state molecular structures

For all compounds except **5-Pr**, single-crystals suitable for X-ray diffraction analysis were grown. These complexes crystallise in the *Sohncke* space groups $P2_1$ or $P2_12_12_1$ in enantiomerically pure form (see Supporting Information); selected bond distances and angles are provided in Table 1. The structural data for **5-La** are too imprecise for the discussion of bond parameters, but the connectivity was qualitatively confirmed by X-ray analysis (see Supporting Information). The following section summarises some of the general features of the solid-state molecular structures:

(1) In line with the lanthanide contraction,[11] early and larger lanthanides (M = La, Ce, Nd) form C_2-symmetric, dimeric complexes with two bridging halide atoms. Therefore, it is reasonable to assume that **5-Pr** also features an analogous structural motif. In these molecules, the pdl ligand coordinates in η^5-*U*-fashion from its sterically less crowded side and the anionic amido function is attached to the metal atom in κ-*N*-mode. Similar structural features are also found for the late lanthanides (M = Gd, Er, Ho, Dy, Tm) and the group 3 metal Y. However, their smaller ionic radii enforce monomeric structures with C_1-symmetry. This is also the case for **6-Sc**, but the pdl fragment switches to the allyl-like η^3-mode, with a double bond between C4 and C5, emphasising the flexibility of this ligand (Figure 5). Therefore, the corresponding Sc–C4 and Sc–C5 bonds are significantly elongated compared to Sc-C1/C2/C3.

(2) The distance of the lanthanide atom from the pdl plane decreases with increasing atomic number from 2.401(1) Å (2.371(1) Å for the second molecule in the asymmetric unit)

Table 1. Selected bond distances [Å] and angles [°] for metal halide compounds **4-M**, **5-M** and **6-Sc**.									
	6-Sc	**4-Y**	**5-Ce**	**5-Nd**	**4-Gd**	**4-Dy**	**4-Ho**	**4-Er**	**4-Tm**
C1–C2	1.382(2)	1.378(5)	1.374(8) [1.368(8)]	1.375(8) [1.378(8)]	1.380(5)	1.386(7)	1.386(3)	1.389(7)	1.391(5)
C2–C3	1.422(2)	1.421(4)	1.421(7) [1.428(8)]	1.422(8) [1.434(8)]	1.424(4)	1.424(6)	1.417(3)	1.424(5)	1.412(4)
C3–C4	1.457(2)	1.437(4)	1.430(7) [1.436(8)]	1.432(7) [1.433(7)]	1.441(5)	1.429(7)	1.440(3)	1.432(6)	1.441(4)
C4–C5	1.358(2)	1.370(4)	1.376(7) [1.375(8)]	1.366(8) [1.371(8)]	1.364(5)	1.381(7)	1.369(3)	1.376(6)	1.372(5)
C1···C5	3.175(2)	3.139(5)	3.183(9) [3.201(8)]	3.167(8) [3.203(9)]	3.143(6)	3.147(8)	3.128(4)	3.134(6)	3.139(5)
M–pdl$_{cent}$	2.177(1)	2.315(1)	2.426(1) [2.402(1)]	2.388(1) [2.373(1)]	2.343(1)	2.318(1)	2.308(1)	2.294(1)	2.290(1)
M–pdl$_{plane}$	2.128(1)	2.301(1)	2.401(1) [2.371(1)]	2.357(1) [2.342(1)]	2.330(1)	2.304(1)	2.296(1)	2.280(1)	2.279(1)
M–C1	2.501(2)	2.802(3)	2.836(6) [2.838(5)]	2.793(5) [2.801(5)]	2.820(4)	2.820(5)	2.795(2)	2.772(5)	2.793(4)
M–C2	2.421(2)	2.651(3)	2.752(5) [2.767(5)]	2.714(5) [2.727(5)]	2.677(3)	2.657(5)	2.643(2)	2.626(4)	2.624(3)
M–C3	2.382(2)	2.597(3)	2.709(5) [2.721(5)]	2.690(5) [2.701(5)]	2.629(3)	2.603(5)	2.591(2)	2.577(4)	2.563(3)
M–C4	2.793(2)	2.783(3)	2.935(5) [2.897(5)]	2.917(5) [2.888(5)]	2.809(3)	2.787(5)	2.781(2)	2.771(4)	2.764(3)
MC–5	3.101(2)	2.968(3)	3.057(6) [2.983(6)]	3.006(5) [2.975(5)]	2.993(3)	2.957(5)	2.964(2)	2.966(4)	2.954(3)
M–N$_{ligand}$	2.035(2)	2.245(3)	2.310(4) [2.314(5)]	2.279(4) [2.289(4)]	2.275(3)	2.243(4)	2.240(2)	2.236(4)	2.227(3)
M–O1 t$_{hf}$	2.172(1)	2.410(2)	2.474(3) [2.577(4)]	2.528(4) [2.521(4)]	2.447(2)	2.423(3)	2.405(2)	2.399(3)	2.388(2)
M–O2 $_{thf}$	–	2.407(2)	–	–	2.443(2)	2.423(3)	2.403(2)	2.390(3)	2.374(2)
M–Cl	2.400(1)	2.626(1)	2.855(2)/2.889(2) [2.864(2)/2.891(2)]	2.832(2)/2.853(2) [2.840(2)/2.852(2)]	2.660(1)	2.630(2)	2.622(1)	2.610(1)	2.596(1)
C1-C2-C3	124.9(2)	125.0(3)	125.3(5) [125.4(5)]	125.1(5) [125.3(5)]	125.4(4)	125.3(5)	125.2(2)	124.8(4)	125.2(3)
C2-C3-C4	128.4(2)	128.9(3)	130.1(5) [129.6(5)]	129.8(5) [129.8(5)]	128.5(3)	128.8(5)	128.7(2)	128.6(4)	129.1(3)
C3-C4-C5	129.8(2)	129.6(3)	129.2(5) [130.2(5)]	129.1(5) [130.1(5)]	129.8(3)	129.7(5)	129.5(2)	129.9(4)	129.1(3)
C13-Si-N1	107.5(1)	107.2(2)	107.0(2) [106.5(3)]	106.7(2) [107.7(2)]	107.5(2)	107.2(2)	107.4(1)	107.4(2)	107.4(2)
Si-N1-M	115.7(1)	120.3(1)	120.3(2) [122.5(3)]	120.5(2) [121.3(2)]	120.2(2)	120.6(2)	119.9(1)	119.6(2)	120.0(2)
pdl$_{cent}$-M-N1	120.3(4)	111.3(1)	106.7(2) [105.5(2)]	107.8(2) [107.7(1)]	110.3(1)	110.8(2)	111.7(5)	112.2(1)	111.9(1)

Chemistry–A European Journal

Full Paper
doi.org/10.1002/chem.202003170

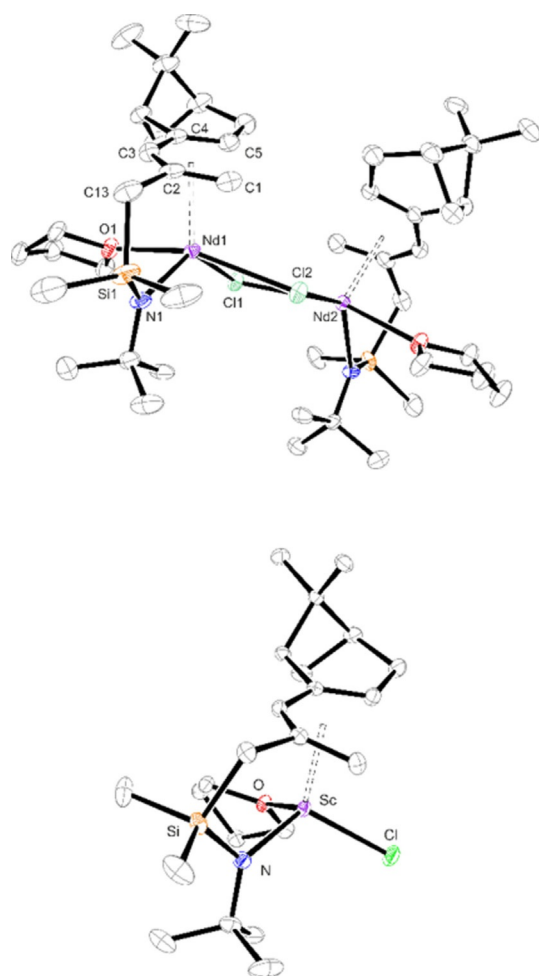**Chemistry Europe**
European Chemical
Societies Publishing

Figure 5. ORTEP drawings of **5-Nd** and **6-Sc**. Thermal ellipsoids are drawn at the 30% probability level. Hydrogen atoms are omitted for clarity. Selected bond lengths and angles are listed in Table 1.

(**5-Ce**) to 2.279(1) Å (**4-Tm**). While Sc as a 3d metal shows the smallest distance, the values for **4-Y** are similar to those of **4-Dy**. A similar trend was also observed for rare-earth metal complexes containing the 2,4-di-*tert*-butylpentadienyl (pdl') ligand[12] and implies ionic rather than covalent metal-ligand interactions in these molecules. This again can be rationalised in terms of the trends in the ionic radii of these elements.[11]

(3) The pdl moiety features the characteristic short-long-long-short bond length pattern that is consistent with previous literature reports.[6a, 7, 13] For the M–C_{pdl} bond distances (with C_{pdl} = C1 to C5), the smallest values are found for M–C3, then increase via M–C2 and M–C1/M–C4 to M–C5. With decreasing

ion radius, the M–C1 and M–C4 distances gradually approach each other. These observations can be rationalised by a predominant localisation of the negative charge on the C3 position. However, in contrast to previous literature reports, in which some charge delocalisation to the C1 and C5 positions is also described,[12, 13c, 14] the asymmetric substitution pattern and the bulkiness of the myrtenal framework enforce a steric repulsion between the pdl ligand and the metal centre.

(4) The bite angle, which is defined as the angle between the pdl plane, the metal atom and the nitrogen atom N1, adopts the largest value for **6-Sc** (ca. 120°). From **5-Ce** to **4-Tm**, this bite angle increases slightly from ca. 108° to 112°, in which the value for **4-Y** coincides with the one found for **4-Ho** and **4-Dy**. This feature can be traced to the very similar radii of these M^{3+} ions.[11] Nevertheless, the significantly increased steric demand of the pdl*-derived ligand results in larger bite angles than the value of 97.1(2)° reported for [(η^5:η^1-$C_5Me_4CH_2$-$SiMe_2NtBu$)Y(CH_2SiMe_3)(thf)].[2a]

NMR spectroscopic studies

The diamagnetic compounds **6-Sc**, **4-Y** and **5-La** were analysed by solution NMR spectroscopy (C_6D_6, $T = 298$ K; Table 2). The NMR data are consistent with C_2- or C_1-symmetric structures, as determined in the solid state. ^1H,^1H NOESY experiments confirmed the *U*-conformation of the pdl ligand in solution by through-space coupling between the H atoms *endo*-H1 and H5. Proton resonances for the pdl moiety are shifted downfield upon coordination to the metal atom and appear between $\delta = 4.20$ ppm and $\delta = 5.65$ ppm. Compounds **5-La** and **4-Y** adopt similar chemical shift patterns, whereby the chemical shift decreases from H5 of the pdl unit via *exo*-H1 and H3 to *endo*-H1. In contrast, the chemical shifts for H3 and H1 are almost identical in **6-Sc**, whereas the H5 resonance is downfield shifted by ca. 0.60 ppm compared to **5-La** and **4-Y**. The methylene protons of the coordinated THF are diastereotopic, as is verified by two broadened resonances for the protons in 2- and 5-position. Addition of a few drops of THF to the NMR sample in C_6D_6 confirmed that no ligand exchange with the solvent occurs on the NMR time scale.

The early lanthanide compounds **5-Ce**, **5-Pr** and **5-Nd**, which exhibit only weak paramagnetism, were examined by ^1H NMR spectroscopy. The relative intensities and number of observed NMR resonances are consistent with their solid-state molecular structures (see Experimental Section and Supporting Information). In contrast, the paramagnetism of the late lanthanide

Table 2. Selected 1H NMR chemical shifts (C_6D_6 or [D8]THF, T = 298 K) for dipotassium salts **3** and **3'** and the diamagnetic lanthanide compounds.

	3 a	3	6-Sc	4-Y	5-La	7-La	7-Y	8-La	9-Lu	10-Lu	11-Lu
exo-H1	–	3.16–3.10	4.20	4.60	4.87	4.86	4.47	4.70	4.54	4.07	3.95
endo-H1	3.19–3.10	3.16–3.10	4.24	4.21	4.34	4.34	4.14	4.08–4.01	4.20	4.15	3.77
H3	3.30	4.52–4.47	4.25	4.30	4.60	4.61	4.27	4.65–4.62	4.10	4.16	4.22
H5	3.76	3.40	5.65	5.08	5.04	5.03	4.83	5.01	5.55	5.68	5.28

Chemistry–A European Journal

Full Paper
doi.org/10.1002/chem.202003170

Chemistry Europe
European Chemical
Societies Publishing

complexes **4-Gd**, **4-Dy**, **4-Ho**, **4-Er** and **4-Tm** prevented useful NMR spectra from being recorded.

Synthesis of rare-earth metal amide complexes

Following the synthesis of metal halide complexes, further functionalisation of these compounds was undertaken by the reaction with lithium bis(trimethylsilyl)amide [Li(N(SiMe$_3$)$_2$)-(OEt$_2$)] in THF at ambient temperature to obtain bis(trimethylsilyl)amide-substituted metal complexes **7-Y**, **7-La**, **7-Nd**, **7-Ho** and **7-Dy** (Figure 4B) as crystalline solids.

Solid-state molecular structures

For **7-Y**, **7-La**, **7-Nd**, **7-Dy** and **7-Ho**, single crystals suitable for X-ray diffraction were obtained. The compounds crystallise in the triclinic space group $P1$ (**7-La**, **7-Nd**) or the monoclinic space group $P2_1$ (**7-Y**, **7-Dy**, **7-Ho**). The C_1-symmetric monomeric structures feature a η^5-U-bonded pdl ligand and one coordinated THF molecule, indicating an increased steric demand of the amido function compared to the halide substituents. As a representative example, **7-Ho** is depicted in Figure 6. For characteristic bond lengths and angles, see Supporting Information Tables S2 and S3. The structural features generally correspond to those of the lanthanide halide complexes described in the previous section. However, a closer examination of the N(SiMe$_3$)$_2$ ligand reveals that the nitrogen atom N2 adopts a pseudo-trigonal-planar geometry. In addition, silicon atom Si3 lies ca. 0.16 Å to 0.22 Å closer to the metal atom than Si2. Previous reports attributed this feature to interactions between empty orbitals of the electron-deficient metal atoms and Si$_\beta$—C$_\gamma$H or Si$_\beta$C$_\gamma$—H bonds.[15] However, more recent studies unambiguously demonstrate that this structural feature can be traced to 3-center-2-electron β-Si-γ-C···Ln interactions[15a] or crystal packing effects that minimise H–H repulsions.[15a, 16]
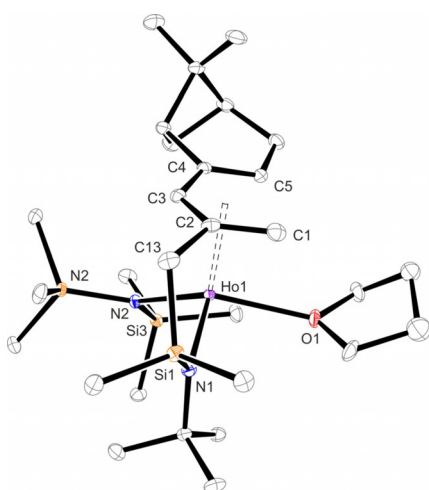

Figure 6. ORTEP drawing of Ho compound **7-Ho**. Thermal ellipsoids are drawn at the 30% probability level. Hydrogen atoms are omitted for clarity. The 3- and 4-positions of the coordinated THF are disordered over two positions, but only one orientation is depicted for clarity.

NMR spectroscopic studies

In addition, the diamagnetic compounds **7-La** and **7-Y** were fully characterised by NMR spectroscopic studies using 2D NMR techniques (see Table 2 and Supporting Information). The resonances match the molecular C_1-symmetry observed in the solid state. However, the N(SiMe$_3$)$_2$ function gives rise to a single resonance with a relative intensity of 18H atoms, indicating that the differences in the M-Si2/3 distances are not preserved in solution.

Synthesis of rare-earth metal tetraborohydride complexes

Organometallic tetraborohydride (BH$_4$) compounds of the rare-earth metals have found numerous applications in coordination chemistry and polymerisation reactions.[17] Nevertheless, the only examples of lanthanide BH$_4$ complexes reported so far that feature a constrained geometry ligand are [(η^5-Me$_4$C$_5$)CH$_2$SiMe$_2$(κ-NPh)Ln((κ-H$_3$)-BH$_4$)(thf)$_2$] (Ln = Nd, Sm).[18] To expand this series we synthesised complexes **8-La** and **8-Nd** by reaction of the corresponding lanthanide BH$_4$ precursor with ligand **3** (Figure 4C) in THF at ambient temperature.

Solid-state molecular structures

Both compounds possess C_2-symmetry and crystallise in the orthorhombic space group $P2_12_12_1$, exhibiting a dimeric structure motif with two bridging BH$_4$ units. The H atoms of the BH$_4$ groups were identified in the Fourier difference map and refined isotropically. **8-La** is depicted in Figure 7, with selected bond lengths and angles provided in Table 3. As the structural data agree with the trends previously observed for the other complexes, only the M–BH$_4$ coordination mode will be discussed in more detail. The BH$_4$ units bind in two different modes to the respective metal atoms. For boron atom B1, the BH$_4$ group coordinates in μ-H$_2$- and κ-H$_2$-fashion. H atoms H01B and H01D are bound to one lanthanum atom each (La1 and La2, respectively), whereas H02A and H01C both bridge La1 and La2. The coordination modes for the second BH$_4$ group are μ-H (H02C) bridging M1 and M2 and κ-H$_2$ (H02A, H02B). The final H atom (H02D) is positioned along the B1–B2 axis. This particular coordination behaviour of two BH$_4$ groups bridging two rare-earth metals in (μ-H$_2$/κ-H$_2$)-(μ-H/κ-H$_2$) mode has not been observed before, although the (μ-H$_2$/κ-H$_2$) binding mode is well-established.[19] Indeed, a similar structural motif was reported for mixed lanthanide-lithium complexes bearing guanidinate ligands,[20] where two BH$_4$ units bridge a lanthanide and a lithium atom in (μ-H$_2$,κ-H)/(μ-H,κ-H$_2$)- (Nd, Sm) and (μ-H$_2$,κ-H)/(κ-H$_3$)-mode (Yb), respectively. In contrast to **8-La** and **8-Nd**, the fourth H atom does not participate in the coordination to the metal atoms. The M–H bond distances in **8-La** lie between 2.51(6) and 2.83(4) Å and do not differ significantly from the values found for **8-Nd** within the standard deviations. They are also in good agreement with other Nd-BH$_4$ complexes reported in literature.[17b, 21] The M–B bond distances of both compounds lie in the range of literature-report-

Chemistry–A European Journal

Full Paper
doi.org/10.1002/chem.202003170

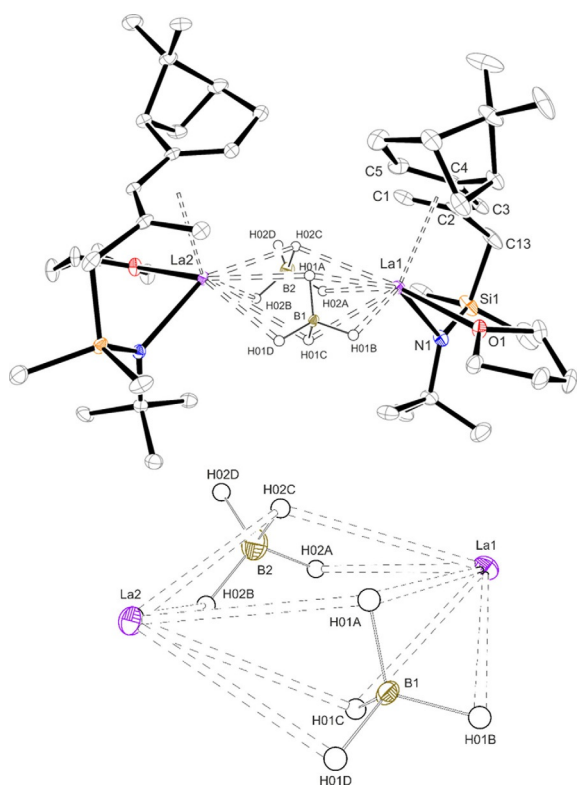**Chemistry Europe**
European Chemical
Societies Publishing

Figure 7. ORTEP drawing of **8-La**. Thermal ellipsoids are drawn at the 30% probability level. Except for the BH$_4$ units, hydrogen atoms are omitted for clarity.

Table 3. Selected bond lengths [Å] and angles [°] for compounds **8-La** and **8-Nd**.[a]

	8-La	8-Nd
C1–C2	1.373(9) [1.367(8)]	1.376(6) [1.371(6)]
C2–C3	1.420(7) [1.428(8)]	1.422(5) [1.421(6)]
C3–C4	1.435(7) [1.434(8)]	1.436(5) [1.433(5)]
C4–C5	1.361(8) [1.373(8)]	1.364(5) [1.373(5)]
C1···C5	3.172(9) [3.195(8)]	3.172(6) [3.184(5)]
M–pdl$_{cent}$	2.448(1) [2.443(1)]	2.385(1) [2.383(1)]
M–pdl$_{plane}$	2.425(1) [2.415(1)]	2.361(1) [2.353(1)]
M–C1	2.854(6) [2.850(6)]	2.792(4) [2.785(4)]
M–C2	2.760(5) [2.784(5)]	2.709(3) [2.724(4)]
M–C3	2.728(5) [2.748(5)]	2.669(3) [2.687(4)]
M–C4	2.953(5) [2.928(6)]	2.904(3) [2.887(4)]
M–C5	3.018(6) [3.062(6)]	3.038(4) [3.024(4)]
M–N$_{ligand}$	2.346(4) [2.345(5)]	2.290(3) [2.288(3)]
M–O1 t$_{hf}$	2.631(3) [2.617(4)]	2.568(2) [2.571(3)]
M1–B1	2.899(5) [2.907(6)]	2.890(4) [2.869(4)]
M1–B2	3.073(6) [3.082(7)]	3.007(5) [3.013(5)]
M2–B1	2.907(5) [2.884(6)]	2.899(5) [2.836(4)]
M2–B2	3.109(6) [3.121(7)]	3.056(5) [3.092(5)]
H01A–M1	2.65(5) [2.60(7)]	2.57(6) [2.55(5)]
H01A–M2	2.83(4) [2.67(6)]	2.89(5) [2.62(4)]
H01B–M1	2.80(6) [2.86(6)]	3.00(6) [2.78(4)]
H01C–M1	2.79(4) [2.76(6)]	2.71(4) [2.79(4)]
H01C–M2	2.62(5) [2.73(6)]	2.61(4) [2.62(4)]
H01D–M2	2.72(6) [2.63(6)]	2.60(5) [2.59(5)]
H02A–M1	2.51(6) [2.53(5)]	2.45(5) [2.42(5)]
H02B–M2	2.58(6) [2.61(5)]	2.47(5) [2.51(5)]
H02C–M1	2.71(5) [2.76(4)]	2.62(4) [2.69(4)]
H02C–M2	2.77(5) [2.78(4)]	2.76(5) [2.72(4)]
C1-C2-C3	126.0(5) [126.0(5)]	125.6(4) [124.8(4)]
C2-C3-C4	129.0(5) [129.5(5)]	129.1(4) [130.1(4)]
C3-C4-C5	129.6(5) [129.8(5)]	129.6(3) [130.0(4)]
C13-Si-N1	106.9(2) [107.2(3)]	106.3(2) [107.2(2)]
Si-N1-M	120.4(2) [121.5(3)]	120.5(2) [121.3(2)]
pdl$_{cent}$-M-N1	105.3(2) [105.3(1)]	106.7(1) [107.0(1)]

[a] Values in square brackets are given for the second molecule in the asymmetric unit.

ed compounds featuring bridging BH$_4$ groups,[17g,18,19a,22] but are longer than in species with terminal BH$_4$ ligands.[17b-e,21,23]

Because of the lanthanide contraction,[11] the M–B bond distances are slightly smaller for the Nd derivative. Compared to the constrained geometry Nd compound mentioned above,[18] these bonds are ca. 0.2–0.3 Å longer, which may be attributed to the different coordination modes of the BH$_4$ units. In contrast, the Nd–Cp/pdl$_{plane}$ distance is shortened by ca. 0.06 Å for the pdl complex Nd-BH4 with respect to the Cp derivative.

In addition, crystalline material of **8-La** and **8-Nd** suspended in Nujol mineral oil was used to record FTIR spectra, which show vibrational bands at ca. 2400–2200 cm^{-1} for the B–H stretching modes and several bands in the region for deformation modes (1250–850 cm^{-1}).[17a,24]

NMR spectroscopic studies

Solution NMR spectroscopy was conducted for both complexes (see Table 2 and Supporting Information). For the diamagnetic compound **8-La**, the observed resonances are consistent with the solid-state molecular structure. Although the ^{1}H NMR resonances for the BH$_4$ ligand were not observed, probably because of significant broadening, a sharp resonance is observed at $\delta = -24.1$ ppm in its ^{11}B{^{1}H} NMR spectrum. The analysis of the paramagnetic **8-Nd** was limited to ^{1}H and ^{11}B{^{1}H} NMR spectroscopy, for which the number of resonances observed in the NMR spectra is consistent with the solid-state molecular structure. Compared to the diamagnetic **8-La**, the

signal in the ^{11}B{^{1}H} NMR spectrum is significantly broadened and shifted downfield to $\delta = 149$ ppm, in line with previous studies on paramagnetic lanthanide BH$_4$ compounds.[17b,22]

Synthesis of lutetium triflate and alkyl complexes

Considering that organometallic rare-earth metal alkyl complexes have proved to be efficient catalysts in numerous transformations[25] including olefin polymerisation,[26] CH bond activation,[27] and hydroamination,[28] we were interested in the synthesis of enantiomerically pure alkyl derivatives featuring the constrained geometry ligand. Unfortunately, the treatment of **6-Sc** with [Mg(CH$_2$SiMe$_3$)$_2$] only affords the ate-complex [((η^3)-pdl*SiMe$_2$NtBu)Sc(Cl)(CH$_2$SiMe$_3$)][MgCl$_2$(thf)$_6$], which led us to focus on the preparation of the trifluoromethanesulfonate-(triflate, OTf) bridged **9-Lu** derivative (Figure 4D). Subsequent treatment of this compound with magnesium dialkyls [Mg(CH$_2$CMe$_3$)$_2$] and [Mg(CH$_2$CMe$_2$Ph)$_2$] gives the desired alkyl compounds **10-Lu** and **11-Lu** (Figure 4E).

Chemistry–A European Journal

Full Paper
doi.org/10.1002/chem.202003170

Chemistry Europe
European Chemical
Societies Publishing

Solid-state molecular structures

Single-crystal X-ray analysis provided solid-state molecular structures of all three compounds. Relevant bond lengths and angles are provided in Table 4. The compounds **9-Lu** and **11-Lu** crystallise in the orthorhombic space group $P2_12_12_1$, whereas **10-Lu** crystallises in the monoclinic space group $P2_1$. The molecular structure of **10-Lu** is shown in Figure 8. While **9-Lu** exhibits a dimeric, C_2-symmetric structure with bridging OTf groups, both alkyl substituted compounds form monomeric structures with C_1-symmetry. The metal-pdl distances are shorter than the aforementioned rare-earth metal complexes, except for **6-Sc**. These observations are consistent with the lanthanide contraction and emphasise the ionic bonding in these compounds. Furthermore, the C—C bond distances within the pdl moiety show a short-long-long-short pattern. In both cases, the Lu-C$_{\text{alkyl}}$ distance is 2.388 Å and thus lies in the range of other reported Lu-alkyl bond distances.[29]
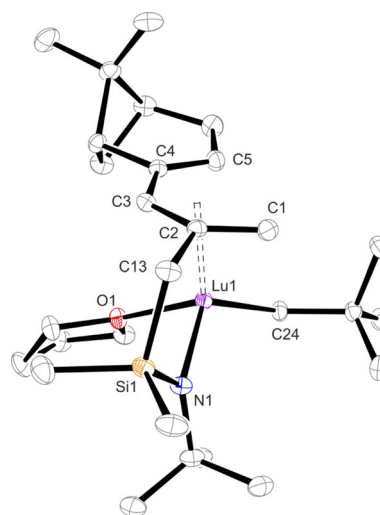

Figure 8. ORTEP drawing of **10-Lu**. Thermal ellipsoids are drawn at the 30% probability level. Hydrogen atoms are omitted for clarity. The 3- and 4-positions of the coordinated THF are disordered over two positions, but only one orientation is depicted for clarity.

Table 4. Selected bond lengths [Å] and angles [°] for Lu compounds **9-Lu**, **10-Lu** and **11-Lu** (X=OTf, C$_{\text{alkyl}}$).			
	9-Lu	**10-Lu**	**11-Lu**
C1—C2	1.367(9)	1.377(8)	1.381(4)
C2—C3	1.428(8)	1.423(7)	1.418(4)
C3—C4	1.450(8)	1.445(6)	1.441(3)
C4—C5	1.373(8)	1.375(7)	1.367(4)
C1···C5	3.140(9)	3.135(7)	3.156(5)
Lu—pdl$_{\text{cent}}$	2.266(1)	2.250(1)	2.230(1)
Lu—pdl$_{\text{plane}}$	2.244(1)	2.219(1)	2.190(1)
Lu—C1	2.679(6)	2.651(5)	2.634(3)
Lu—C2	2.571(5)	2.576(5)	2.578(3)
Lu—C3	2.518(6)	2.564(5)	2.579(3)
Lu—C4	2.816(6)	2.800(4)	2.791(3)
Lu—C5	3.009(7)	2.936(5)	2.874(3)
Lu—N$_{\text{ligand}}$	2.166(4)	2.199(4)	2.201(2)
Lu—O1 t$_{\text{hf}}$	2.361(4)	2.278(3)	2.272(2)
Lu—X	2.303(3)/2.331(4)	2.388(5)	2.388(3)
C1-C2-C3	125.1(5)	125.2(5)	125.9(3)
C2-C3-C4	128.3(5)	128.2(4)	129.2(2)
C3-C4-C5	128.9(6)	129.4(4)	128.6(3)
C13-Si-N1	105.8(2)	108.5(2)	108.3(2)
Si-N1-Lu	118.7(2)	117.4(2)	116.0(2)
pdl$_{\text{cent}}$-Lu-N1	115.0(2)	113.3(2)	111.7(7)

NMR spectroscopic studies

Full characterisation of the Lu complexes was achieved by solution NMR spectroscopy. Figure 9a shows the ^{1}H NMR spectrum of **10-Lu** with the assigned resonances. In agreement with the C_1-symmetry of this molecule, the THF protons oriented towards or away from the pdl ligand are diastereotopic, thus giving rise to two resonances. The same is observed for the proton signals 13a/b, 14/15 and 16a/b. The metal bound methylene group features two high-field shifted resonances at $\delta = 0.45$ ppm and $\delta = 0.34$ ppm with a $^2J_{\text{H,H}}$ coupling constant of 14.5 Hz. The ^{1}H,^{1}H NOESY NMR spectrum is depicted in Figure 9b. As expected from the molecular structure with a η^5-U-coordinated pdl moiety, through-space cross peaks between endo-H1/H5, H3/H13b and H8b/H12 are found. Similar spectro-

scopic data can also be obtained for **9-Lu** and **11-Lu** (see Table 2 and Supporting Information).

Conclusions

To the best of our knowledge, we present the first examples of enantiomerically pure rare-earth metal complexes featuring a dianionic constrained geometry ligand, which consists of a pdl moiety (π-donor), a dimethylsilyl methylene group (bridge) and a tert-butylamido function (σ-donor). These complexes were synthesised by reaction of the dipotassium salt [K$_2$(pdl*SiMe$_2$NtBu)] (**3**) with suitable metal precursors. In all isolated complexes, the coordination to the metal atom occurs both through the pdl and the amide function, resulting in the formation of monomeric C_1- or dimeric C_2-symmetric products. A prerequisite for the formation of these compounds is the 1,3-H shift of **3**, occurring in solution, which elongates the bridge by one CH$_2$ group and therefore allows the formation of the constrained geometry complexes. The rare-earth metal compounds were extensively characterised by solid-state X-ray diffraction analysis and solution NMR spectroscopy. Further investigations on the reactivity in enantioselective catalysis and magnetic properties of the paramagnetic compounds are currently ongoing and will be reported in due course.

Experimental Section

General Considerations

All syntheses were carried out under inert conditions using a glovebox (Unilab by MBraun) or standard Schlenk techniques with an N$_2$ atmosphere. Solvents were dried over Na/benzophenone, distilled and degassed. Lanthanide trifluoromethanesulfonates were synthesised starting from the corresponding lanthanide oxides (Ln$_2$O$_3$) and sub-stoichiometric amounts of trifluoromethanesulfonic acid. The resulting [Ln(OTf)$_3$(H$_2$O)$_x$] complexes were dried in dy-

Chemistry–A European Journal

Full Paper
doi.org/10.1002/chem.202003170
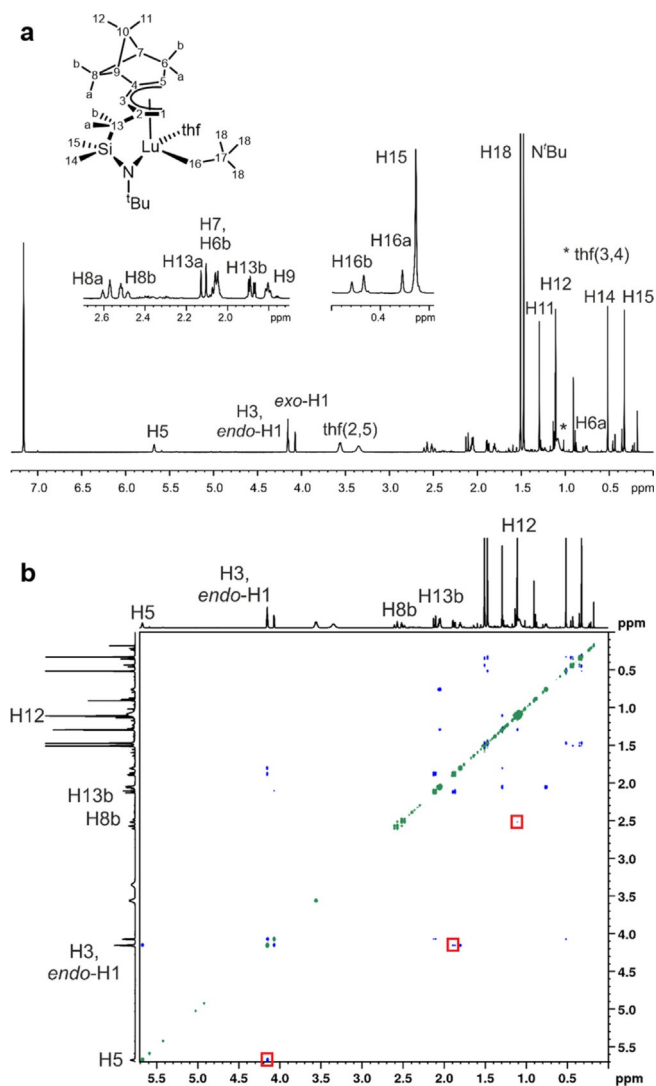
Chemistry
Europe
European Chemical
Societies Publishing

Figure 9. ^{1}H NMR spectrum (a; 500 MHz, C_6D_6) and ^{1}H,^{1}H NOESY experiment (b) of **10-Lu** with assigned proton signals and relevant cross peaks marked in red.

Figure 10. General labelling scheme for the reported compounds.

Elemental analyses were recorded using the Vario-Micro-Cube-System. Despite several attempts, we did not succeed in obtaining satisfactory elemental analyses data for some of the compounds described below. This can be traced to either partial loss of coordinated solvents or the high air- and moisture-sensitivity. Similar observations for other organometallic rare-earth metal complexes have previously been described in the literature.[6b, 14, 22, 26a, 34] Furthermore, we provided some explanations in the experimental section below where necessary. Melting points were determined visually with the melting point meter MPM-HV2. Infrared (IR) spectra were measured on a Bruker Vertex 70 FTIR with the sample suspended in Nujol and placed between two KBr discs. Signals were classified as medium (m), weak (w) and broad (br).

Crystals for X-ray diffraction analysis were mounted on glass fibers or hairs in inert oil. Data were collected on Oxford Diffraction systems using mirror-focussed Cu-K_α or monochromated (in some cases mirror-focussed) Mo-K_α radiation. Structures were refined anisotropically against F^2 using SHELXL-2017.[35] Hydrogen atoms were added using rigid methyl groups or the riding model. H atoms of the positions C1, C3 and C5 of the pentadienyl moiety were usually refined freely (for details and exceptions see the Supporting Information). Deposition numbers 2013843 (6-Sc), 2013844 (4-Y), 2013845 (4-Y*), 2013846 (5-Ce), 2013847 (5-Nd), 2013848 (4-Gd), 2013849 (4-Dy), 2013850 (4-Ho), 2013851 (4-Er), 2013682 (4-Tm), 2013683 (4-Tm*), 2013684 (7-Y), 2013685 (7-La), 2013686 (7-Nd), 2013687 (7-Dy), 2013688 (7-Ho) 2013689 (8-La), 2013690 (8-Nd), 2013691 (9-Lu), 2013695 (10-Lu), and 2013696 (11-Lu) contain the supplementary crystallographic data for this paper. These data are provided free of charge by the joint Cambridge Crystallographic Data Centre and Fachinformationszentrum Karlsruhe Access Structures service.

Gas chromatographic measurements were carried out on a Shimadzu type GC2010 device. A Zebron ZB-5MS column with helium as carrier gas and an FID detector were employed. The temperature program was set up as follows: starting temperature 50 °C (3 min), heating rate 20 °C min^{-1} to 300 °C, 300 °C (7 min). For gas chromatographic measurements with subsequent mass spectrometry, the device Shimadzu GCMS-QP2010 SE with a ZB-5MS column and a mass detector (EI) were utilised. The following temperature program was applied: starting temperature 50 °C (3 min), heating rate 12 °C min^{-1} to 300 °C, 300 °C (8 min). Retention indices *I* were calculated with the Kováts method.[36]

namic oil pump vacuum until the HO stretching frequency of water could no longer be observed in the IR spectrum. LnCl$_3$ (Ln = La, Nd, Dy, Ho) were dried in THF using thionyl chloride to form the corresponding THF adducts, and the content of coordinated THF was determined by elemental analysis. [LaI$_3$(thf)$_4$],[30] the bis(alkyl) magnesium compounds [Mg(CH$_2$CMe$_3$)$_2$] and [Mg(CH$_2$CMe$_2$Ph)],[31] [KpdI*][8, 10a, b, 32] and ClSiMe$_2$NHtBu[33] were synthesised according to literature procedures. Commercially purchased chemicals were used as received if not otherwise stated. NMR spectra were recorded on Bruker AVII300 (300 MHz), Bruker AVIII400 (400 MHz), Bruker AVIIIHD500 (500 MHz) and Bruker AVII600 (600 MHz) at ambient temperature. For ^{1}H NMR spectra, tetramethylsilane or residual solvent proton signals were used as standards. ^{11}B{^{1}H} NMR spectra were referenced externally with BF$_3$·Et$_2$O. The chemical shift δ and the coupling constants J were given in parts per million (ppm) and Hertz (Hz), respectively. Splitting patterns were assigned as s (singlet), d (doublet), t (triplet), q (quartet), sept (septet), m (multiplet) and br. (broad). For the assignment of NMR resonances, the labelling Scheme shown in Figure 10 is applied.
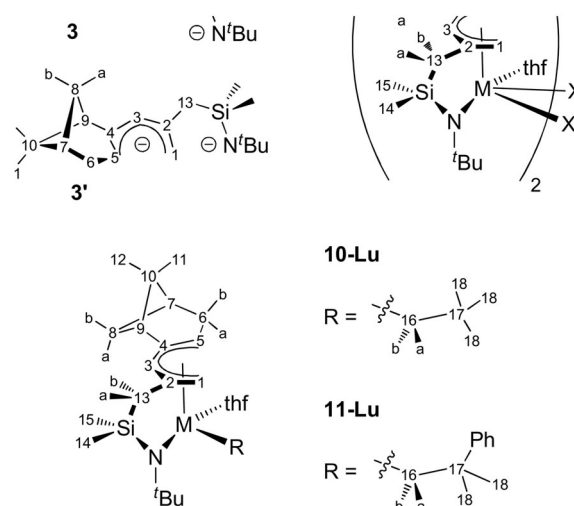
Chemistry–A European Journal

Full Paper
doi.org/10.1002/chem.202003170

Chemistry Europe
European Chemical
Societies Publishing

Procedures

Synthesis of H(pdl*SiMe₂NHtBu) (2): The potassium salt **1** (2.04 g, 9.50 mmol, 1.00 equiv) was dissolved in THF (150 mL) and cooled to −78 °C. ClSiMe₂NHtBu (1.57 g, 9.50 mmol, 1.00 equiv.) was added dropwise and the reaction mixture was allowed to warm up to ambient temperature. After stirring for 4 h, the solvent was removed in vacuum and the red-brown residue was extracted with *n*-hexane (100 mL). After centrifugation (30 min, 3894 *g*, 10 °C), the supernatant liquid was removed, filtered through celite and the solvent removed in vacuum. The residue was distilled under reduced pressure (0.012 mbar, 92 °C) to yield the product as a colourless, air- and moisture-sensitive oil (2.12 g, 6.94 mmol, 73 %). GC/MS (EI): *I* = 1601.99 (*m/z* = 305 amu), *I* = 1629.45 (*m/z* = 305 amu). Anal. calc. (%) for C₁₉H₃₅NSi (305.58 g mol⁻¹) C 74.68, H 11.55; found: C 73.94, H 11.48. The product was formed as a mixture of *s*-cis/trans*-isomers (Figure 11) as previously observed for aminosilyl-pentadienes,[8] which resulted in a duplicated set of NMR resonances. The ratio of 1:0.8 of the isomers **2-cis** and **2-trans** was determined by ¹H NMR spectroscopy. Where possible, signals were assigned and integrated, and the values refer to the single isomers. ¹H NMR (400 MHz, C₆D₆, 298 K): δ = 5.65–5.62 (m), 5.62–5.59 (m), 5.59–5.57 (m), 5.56–5.52 (m), 5.41–5.38 (m), 2.44–2.30 (m), 2.30–2.20 (m), 2.08–2.00 (m), 1.87 (s), 1.86 (s), 1.80 (s), 1.73 (s), 1.68 (s), 1.61 (s), 1.39 (s), 1.37 (s), 1.36 (s), 1.34 (s), 1.33 (s), 1.30 (s), 1.30 (s), 1.28 (s, 3 H, CH₃, 2-trans), 1.27 (s, 3 H, CH₃, 2-trans), 1.25 (s, 3 H, CH₃, 2-trans), 1.12 (s, 9 H, C(CH)₃, 2-trans), 1.11 (s, 9 H, C(CH)₃, 2-cis), 1.00 (s, 3 H, CH₃, 2-cis), 0.99 (s, 3 H, CH₃, 2-cis), 0.96 (s, 3 H, CH₃, 2-cis), 0.69 (br. s, 1 H, NH, 2-trans), 0.55 (br. s, 1 H, NH, 2-cis), 0.22 (s, 6 H, Si(CH₃)₂, 2-trans), 0.16 (s, 3 H, Si(CH₃)₂, 2-cis), 0.16 (s, 3 H, Si(CH₃)₂, 2-cis) ppm. ¹³C{¹H} NMR (101 MHz, C₆D₆, 298 K): δ = 146.3 (C_q), 146.2 (C_q), 135.4 (C_q), 135.0 (C_q), 125.2 (CH), 124.7 (CH), 119.7 (CH), 119.5 (CH), 49.5 (C_q), 49.4 (C_q), 47.8 (CH), 41.1 (CH), 41.1 (CH), 38.1 (C_q), 38.0 (C_q), 34.0 (3 × CH₃, C(CH₃)₃, 2-cis, 2-trans), 33.9 (3 × CH₃, C(CH₃)₃, 2-cis, 2-trans), 33.6 (CH₂), 32.2 (CH₂), 32.2 (CH₂), 32.0 (CH₂), 32.0 (CH₂), 27.4, 26.9 (CH₂), 26.7 (CH₃, 2-trans), 26.7 (CH₃, 2-trans), 26.6 (CH₃, 2-trans), 21.6 (CH₃), 21.5 (CH₃), 21.5 (CH₃), 21.3 (CH₃), 3.0 (CH₃, Si(CH₃)₂, 2-trans), 2.9 (CH₃, Si(CH₃)₂, 2-trans), 2.0 (2 × CH₃, Si(CH₃)₂, 2-cis) ppm.

Synthesis of [K₂(pdl*SiMe₂NtBu)] (3): KOtPen (1.65 g, 13.1 mmol, 2.00 equiv) was suspended in *n*-hexane (100 mL) and cooled to −78 °C. *n*BuLi (8.2 mL, 13.1 mmol, 2.00 equiv., 1.6 M in *n*-hexane) was added dropwise and the reaction mixture was stirred at low temperature for 10 min. The aminosilylpentadiene **2** (2.00 g, 6.54 mmol, 1.00 equiv.) was then added. The reaction mixture was stirred for 30 min at −78 °C and for another 2 h after warming to 0 °C. The cold suspension was then filtered, and the yellow solid was washed with cold *n*-hexane (3×15 mL). After drying in vacuum, the product was obtained as a yellow, pyrophoric solid (2.24 g, 5.87 mmol, 90 %). Anal. calc. (%) for C₁₉H₃₃NSiK₂ (381.39 g mol⁻¹) C 59.78, H 8.71; found: C 59.11, H 8.86. In solution, **3** converts to compound **3′**. Therefore, the NMR spectra always showed a mixture of both isomers. Data for **3**: ¹H NMR (600 MHz,
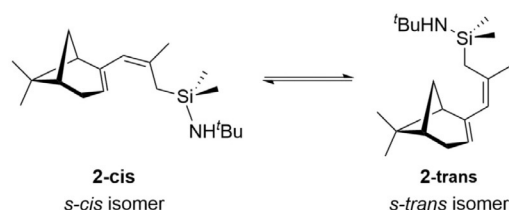
[D₈]THF, 298 K): δ = 3.76 (br. s, 1 H, H5), 3.30 (s, 1 H, H3), 3.19–3.10 (m, 1 H, H1), 2.59 (dt, J_H,H = 15.7, 2.8 Hz, 1 H, H6), 2.50 (dt, J_H,H = 15.7, 2.8 Hz, 1 H, H6), 2.30 (dt, J_H,H = 8.1, 5.8 Hz, 1 H, H8b), 2.06 (sept, J_H,H = 3.0 Hz, 1 H, H7), 1.84 (t, 1 H, J_H,H = 5.5 Hz, H9), 1.73 (s, 3 H, 13-CH₃), 1.22 (s, 3 H, H12), 1.20 (s, 1 H, H8a), 1.10 (s, 9 H, C(CH₃)₃), 0.95 (s, 3 H, H11), −0.08 (s, 3 H, Si(CH₃)₂, −0.10 (s, 3 H, Si(CH₃)₂) ppm. ¹³C{¹H} NMR (151 MHz, [D₈]THF, 298 K): δ = 149.7 (C_q, C2), 149.2 (C_q, C4), 83.8 (CH, C3), 82.4 (CH, C5), 75.7 (CH, C1), 54.1 (CH, C9), 49.5 (C_q, C(CH₃)₃), 42.4 (CH, C7), 39.0 (CH₃, C(CH₃)₃), 38.9 (C_q, C10), 33.1 (CH₂, C6), 33.1 (CH₂, C8), 27.7 (CH₃, C13), 27.2 (CH₃, C12), 22.1 (CH₃, C11), 7.6 (CH₃, Si(CH₃)₂), 7.5 (CH₃, Si(CH₃)₂) ppm. Data for **3′**: ¹H NMR (600 MHz, [D₈]THF, 298 K): δ = 4.52–4.47 (m, 1 H, H3), 3.40 (s, 1 H, H5), 3.16–3.10 (m, 2 H, H1), 2.53 (dt, J_H,H = 16.1, 3.2 Hz, 1 H, H6), 2.43 (dt, J_H,H = 16.1, 3.2 Hz, 1 H, H6), 2.27 (dt, J_H,H = 8.1, 5.7 Hz, 1 H, H8b), 2.03 (sept, J_H,H = 2.9 Hz, 1 H, H7), 1.90 (s, 1 H, H13), 1.89–1.87 (m, 1 H, H13), 1.77 (J_H,H = 5.7 Hz, 1 H, H9), 1.27 (d, J_H,H = 8.1 Hz, 1 H, H8a), 1.21 (s, 3 H, H12), 1.14 (s, 9 H, C(CH₃)₃), 0.91 (s, 3 H, H11), 0.08 (s, 3 H, Si(CH₃)₂), 0.06 (s, 3 H, Si(CH₃)₂) ppm. ¹³C{¹H} NMR (151 MHz, [D₈]THF, 298 K): δ = 151.1 (C_q, C4), 149.6 (C_q, C2), 90.8 (CH, C5), 89.4 (CH, C3), 78.6 (CH₂, C1), 54.0 (CH, C9), 49.5 (C_q, C(CH₃)₃), 42.4 (CH, C7), 38.8 (C_q, C10), 34.3 (CH₃, C(CH₃)₃), 33.0 (CH₂, C6), 32.9 (CH₂, C8), 27.3 (CH₂, C13), 27.3 (CH₃, C12), 21.6 (CH₃, C11), 5.9 (CH₃, Si(CH₃)₂), 5.9 (CH₃, Si(CH₃)₂) ppm.

General procedure for the synthesis of rare-earth metal halide complexes 4-M, 5-M and 6-Sc: The appropriate rare-earth metal salt [LnCl₃(thf)_n] (1.00 equiv.) was suspended in THF (30 mL) inside a glovebox. Then, a solution of [K₂(pdl*SiMe₂NtBu)] (**3**; 1.00 equiv.) was added dropwise and the reaction mixture was stirred at ambient temperature. The solvent was removed under reduced pressure and the residue was extracted with *n*-hexane (60 mL). The resulting suspension was centrifuged (30 min, 3894 *g*, 10 °C) and the supernatant solution was filtered through glass wool and celite. After removal of the solvent, the crude product was purified in the work-up procedure including crystallisation or precipitation, washing of the resulting solid and drying in vacuum.

Complex **5-La** was synthesised by a similar procedure starting from [LaI₃(thf)₄]. After completion of the reaction, the solvent was removed under reduced pressure. The residue was suspended in *n*-hexane/THF (2:1), centrifuged (30 min, 3894 *g*, 10 °C) and the supernatant liquid was filtered through glass wool and celite. Removal of the solvent resulted in the formation of a yellow foam, which was stirred in *n*-hexane (5 mL) for 2 h. The yellow precipitate was washed with Et₂O and further purified.

Individual information regarding the purification process of each compound can be found in Table 5. Spectroscopic data are listed below.

6-Sc. Yield: Yellow crystals; 97 mg (0.213 mmol, 20 %). Mp.: 113 °C (rev.). Anal. calc. (%) for C₂₃H₄₁NOSiClSc (456.08 g mol⁻¹) C 60.57, H 9.06, N 3.07; C₁₉H₃₃NSiClSc (loss of one coordinated THF molecule) C 59.43, H 8.66, N 3.65; found C 59.88, H 8.86, N 3.07. Because of THF loss and the high air- and moisture-sensitivity, these are the best values obtained. Nevertheless, the NMR spectra provided in the Supporting Information are (within the NMR detection limits) in agreement of a pure product. ¹H NMR (500 MHz, C₆D₆, 298 K): δ = 5.65 (s, 1 H, H5), 4.25 (s, 1 H, H3), 4.24 (s, 1 H, endo-H1), 4.20 (s, 1 H, exo-H1), 3.78–3.69 (m, 2 H, thf(2,5)), 3.68–3.59 (m, 2 H, thf(2,5)), 2.58 (m, 1 H, H6a), 2.39 (m, 1 H, H6b), 2.28 (s, 1 H, H8b), 2.22–2.13 (d, 1 H, ²J_H,H = 12.1 Hz, H13a), 2.04 (sept, 1 H, ⁴J_H,H = 2.5 Hz, H7), 1.99–1.82 (m, 2 H, H9, H13b), 1.48 (s, 1 H, H8b), 1.47 (s, 9 H, NC(CH₃)₃), 1.28 (s, 3 H, H12), 1.16–1.11 (m, 4 H, thf(3,4)), 1.00 (s, 3 H, H11), 0.44 (s, 3 H, H14), 0.30 (s, 3 H, H15) ppm. ¹³C{¹H} NMR (126 MHz, C₆D₆, 298 K): δ = 157.8 (C_q, C2), 145.4 (C_q, C4), 109.9 (CH, C5), 96.2 (CH, C3), 85.4 (CH₂, C1), 73.0 (2 × CH₂, thf(2,5)), 55.8 (C_q, NC(CH₃)₃), 51.6

Figure 11. Isomers formed during the synthesis of **2**.

2-cis
s-cis isomer

2-trans
s-trans isomer

Chemistry–A European Journal

Full Paper
doi.org/10.1002/chem.202003170

**Chemistry
Europe**
European Chemical
Societies Publishing

Table 5. Detailed reaction times and purification methods for halide complexes.

Compound	Precursor	M [g mol^{-1}]	n [mmol]	Reaction time	Washing	Crystallisation conditions
6-Sc	[ScCl$_3$(thf)$_3$]	367.96	1.05	3 h	n-hexane	n-hexane
4-Y	YCl$_3$	195.26	1.05	2 h	n-hexane	THF/n-hexane, −30 °C
5-La	[LaI$_3$(thf)$_4$]	808.05	0.787	2 h	n-hexane	Et$_2$O, −30 °C
5-Ce	[CeCl$_3$(thf)$_3$]	462.95	1.05	18 h	n-hexane	THF/HMDSO, rt
5-Pr	PrCl$_3$	247.27	1.05	18 h	n-hexane	THF/n-hexane, rt
5-Nd	[NdCl$_3$(thf)]	393.49	1.31	18 h	–	THF/n-hexane, rt
4-Gd	GdCl$_3$	263.60	0.787	24 h	–	THF/n-hexane, rt
4-Dy	[DyCl$_3$(thf)$_3$]	485.19	1.05	18 h	n-hexane	THF or n-hexane, rt
4-Ho	[HoCl$_3$(thf)$_3$]	521.74	1.05	18 h	THF	THF, rt or n-hexane, −30 °C
4-Er	ErCl$_3$	273.62	0.787	3 h	–	THF/ n-hexane, −30 °C
4-Tm	TmCl$_3$	275.28	0.787	24 h	–	THF/n-hexane, rt

(CH, C9), 40.8 (CH, C7), 38.3 (C$_q$, C10), 34.9 (CH$_2$, C13), 34.9 (3 × CH$_3$, NC(CH$_3$)$_3$), 32.7 (CH$_2$, C6), 31.8 (CH$_2$, C8), 26.6 (CH$_3$, C12), 25.1 (2 × CH$_2$, thf(3,4)), 21.2 (CH$_3$, C11), 7.0 (2 × CH$_3$, C14, C15) ppm. **4-Y**.[37] Yield: Yellow crystals; 153 mg (0.267 mmol, 25%). Mp.: 180 °C. Anal. calc. (%) for C$_{23}$H$_{41}$NOSiClY (572.13 g mol^{-1}) C 56.68, H 8.63, N 2.45; found C 56.34, H 8.76, N 2.87. ^{1}H NMR (400 MHz, C$_6$D$_6$, 298 K): δ = 5.08 (br. s, 1 H, H5), 4.60 (s, 1 H, exo-H1), 4.30 (s, 1 H, H3), 4.21 (s, 1 H, endo-H1), 3.92–3.79 (m, 4 H, thf(2,5)), 3.74–3.63 (m, 4 H, thf(2,5)), 3.20–2.99 (m, 1 H, H6b), 2.76–2.48 (m, 1 H, H6a), 2.23–2.06 (m, 3 H, H7, H8b), 2.16 (d, 1 H, J$_{H,H}$ = 12.8 Hz, H13), 1.95 (t, 1 H, J$_{H,H}$ = 5.3 Hz, H9), 1.81 (d, 1 H, J$_{H,H}$ = 11.0 Hz, H13), 1.52 (s, 10 H, H8a, NC(CH$_3$)$_3$), 1.38–1.29 (m, 8 H, thf(3,4)), 1.34 (s, 3 H, H12), 1.13 (s, 3 H, H11), 0.54 (s, 3 H, 14-Si(CH$_3$)$_2$), 0.30 (s, 3 H, 15-Si(CH$_3$)$_{2)}$ ppm. ^{13}C{^{1}H} NMR (101 MHz, C$_6$D$_6$, 298 K): δ = 153.1 (C$_q$, C4), 148.5 (C$_q$, C2), 99.7 (CH, C5), 89.8 (CH, C3), 88.3 (CH$_2$, C1), 70.5 (2 × CH$_2$, thf(2,5)), 54.4 (C$_q$, NC(CH$_3$)$_3$), 52.3 (CH, C9), 41.3 (CH, C7), 38.9 (C$_q$, C10), 34.8 (CH$_2$, C13), 34.4 (3 × CH$_3$, NC(CH$_3$)$_3$), 32.5 (CH$_2$, C6), 30.5 (CH$_2$, C8), 26.6 (CH$_3$, C12), 25.5 (2 × CH$_2$, thf(3,4)), 21.3 (CH$_3$, C11), 8.0 (CH$_3$, 14-Si(CH$_3$)$_2$), 7.6 (CH$_3$, 15-Si(CH$_3$)$_2$) ppm. **5-La**. Yield: Yellow crystals or powder; 192 mg (0.150 mmol, 38%). Mp.: 155 °C (rev). Anal. calc. (%) for C$_{46}$H$_{82}$Si$_2$N$_2$O$_2$I$_2$La$_2$ (1282.96 g mol^{-1}) C 43.06, H 6.44, N 2.18; C$_{38}$H$_{66}$Si$_2$N$_2$I$_2$La$_2$ (loss of two coordinated THF molecules) C 40.08, H 5.84, N 2.46; found C 40.25, H 6.04, N 1.63. Because of the high air- and moisture-sensitivity of this compound and its susceptibility to THF loss, these values are the results we could achieve. However, the NMR spectra provided in the SI are (within the NMR detection limits) in agreement of a pure product. ^{1}H NMR (400 MHz, C$_6$D$_6$, 298 K): δ = 5.04 (br. s, 1 H, H5), 4.87 (br. s, 1 H, exo-H1), 4.60 (br. s, 1 H, H3), 4.34 (br. s, 1 H, endo-H1), 4.05–3.87 (m, 2 H, thf(2,5)), 3.85–3.69 (m, 2 H, thf(2,5)), 3.16 (br. d, ^{2}J$_{H,H}$ = 15.5 Hz, 1 H, H6a), 2.72 (br. d, ^{2}J$_{H,H}$ = 15.5 Hz, 1 H, H6b), 2.27 (br. s, 1 H, H13), 2.15 (br. d, 2 H, H7, H8b), 2.06 (br. s, 1 H, H9), 1.76 (br. s, 2 H, H8a, H13), 1.58 (s, 9 H, NC(CH$_3$)$_3$), 1.33–1.26 (m, 4 H, thf(3,4)), 1.30 (s, 3 H, H12), 1.11 (s, 3 H, H11), 0.54 (s, 3 H, H14), 0.24 (s, 3 H, H15) ppm. ^{13}C{^{1}H} NMR (101 MHz, C$_6$D$_6$, 298 K): δ = 154.3 (C$_q$), 151.4 (C$_q$), 100.0 (CH, C5), 96.4 (CH, C3), 92.2 (br. CH$_2$, C1), 72.0 (2 × CH$_2$, thf(2,5)), 55.4 (C$_q$, NC(CH$_3$)$_3$), 52.5 (CH, C9), 41.4 (CH, C7), 39.1 (C$_q$, C10), 34.4 (CH$_2$, C8), 33.5 (3 × CH$_3$, NC(CH$_3$)$_3$), 32.8 (CH$_2$, C6), 31.1 (br. CH$_2$, C13), 26.6 (CH$_3$, C12), 25.3 (2 × CH$_2$, thf(3,4)), 21.4 (CH$_3$, C11), 7.8 (CH$_3$, C14), 6.9 (CH$_3$, C15) ppm. **5-Ce**. Yield: Orange powder; 165 mg (0.150 mmol, 23%). Mp.: 161 °C (rev). Anal. calc. (%) for C$_{46}$H$_{82}$O$_2$N$_2$Si$_2$Cl$_2$Ce$_2$ (1102.48 g mol^{-1}) C 50.12, H 7.50, N 2.54; found C 50.22, H 7.37, N 2.31. ^{1}H NMR (400 MHz, C$_6$D$_6$, 298 K): δ = 21.6 (ν$_{1/2}$ = 35 Hz), 21.2 (ν$_{1/2}$ = 60 Hz), 20.4 (ν$_{1/2}$ = 45 Hz), 18.3 (ν$_{1/2}$ = 15 Hz), 16.1 (ν$_{1/2}$ = 70 Hz), 14.5 (ν$_{1/2}$ = 60 Hz), 12.8 (ν$_{1/2}$ = 50 Hz, 3 H, CH$_3$), 10.9 (ν$_{1/2}$ = 60 Hz, 3 H, CH$_3$), 8.4 (ν$_{1/2}$ = 55 Hz), 6.8 (ν$_{1/2}$ = 40 Hz), 3.9 (ν$_{1/2}$ = 40 Hz), 3.6 (ν$_{1/2}$ = 30 Hz), 3.4 (ν$_{1/2}$ = 7 Hz), 3.2 (ν$_{1/2}$ = 30 Hz), 0.41 (ν$_{1/2}$ = 60 Hz), −0.8 (ν$_{1/2}$ = 10 Hz), −1.7 (ν$_{1/2}$ = 8 Hz), −2.6 (ν$_{1/2}$ =

40 Hz), −3.1 (ν$_{1/2}$ = 40 Hz), −3.7 (ν$_{1/2}$ = 12 Hz), −4.0 (ν$_{1/2}$ = 50 Hz), −7.1 (ν$_{1/2}$ = 120 Hz), −7.1 (ν$_{1/2}$ = 10 Hz), −7.2 (ν$_{1/2}$ = 10 Hz), −8.9 (ν$_{1/2}$ = 40 Hz), −10.8 (ν$_{1/2}$ = 70 Hz), −11.5 (ν$_{1/2}$ = 70 Hz), −16.2 (ν$_{1/2}$ = 75 Hz, 9 H, NC(CH$_3$)$_3$), −23.4 (ν$_{1/2}$ = 30 Hz), −42.6 (ν$_{1/2}$ = 100 Hz) ppm. **5-Pr**. Yield: Orange crystals; 160 mg (0.145 mmol, 37%). Mp.: 178 °C (rev). Anal. calc. (%) for C$_{46}$H$_{82}$Si$_2$N$_2$O$_2$Cl$_2$Pr$_2$ (1103.38 g mol^{-1}) C 50.04, H 7.43, N 2.54; found C 50.29, H 7.77, N 2.54. ^{1}H NMR (300 MHz, [D$_8$]THF, 298 K): δ = 98.0 (ν$_{1/2}$ = 75 Hz), 86.2 (ν$_{1/2}$ = 100 Hz), 61.6 (ν$_{1/2}$ = 100 Hz), 56.9 (ν$_{1/2}$ = 180 Hz), 51.6 (ν$_{1/2}$ = 120 Hz), 34.2 (ν$_{1/2}$ = 90 Hz), 33.3 (ν$_{1/2}$ = 90 Hz, 3 H, CH$_3$), 31.8 (ν$_{1/2}$ = 80 Hz, 3 H, CH$_3$), 25.1 (ν$_{1/2}$ = 80 Hz), 21.1 (ν$_{1/2}$ = 150 Hz), 13.1 (ν$_{1/2}$ = 100 Hz), 8.5 (ν$_{1/2}$ = 100 Hz), 2.6 (ν$_{1/2}$ = 100 Hz), 1.78 (ν$_{1/2}$ = 70 Hz), 1.34 (s), −9.0 (ν$_{1/2}$ = 60 Hz), −22.0 (ν$_{1/2}$ = 50 Hz), −23.2 (ν$_{1/2}$ = 70 Hz, 9 H, NC(CH$_3$)$_3$), −53.3 (ν$_{1/2}$ = 70 Hz), −94.7 (ν$_{1/2}$ = 90 Hz), −99.2 (ν$_{1/2}$ = 70 Hz), −106.4 (ν$_{1/2}$ = 170 Hz) ppm. **5-Nd**. Yield: Green-red crystals (dichroic); 221 mg (0.199 mmol, 30%). Mp.: 120 °C (rev). Anal. calc. (%) for C$_{46}$H$_{82}$O$_2$N$_2$Si$_2$Cl$_2$Nd$_2$ (1110.73 g mol^{-1}) C 49.74, H 7.44, N 2.52; found C 49.97, H 7.23, N 2.32. ^{1}H NMR (300 MHz, C$_6$D$_6$, 298 K): δ = 55.3 (ν$_{1/2}$ = 80 Hz), 33.8 (ν$_{1/2}$ = 120 Hz), 29.5 (ν$_{1/2}$ = 230 Hz), 17.8 (ν$_{1/2}$ = 70 Hz), 16.7 (ν$_{1/2}$ = 25 Hz, 3 H, CH$_3$), 14.3 (ν$_{1/2}$ = 25 Hz, 3 H, CH$_3$), 12.7 (ν$_{1/2}$ = 75 Hz), 11.0 (ν$_{1/2}$ = 35 Hz), 6.7 (ν$_{1/2}$ = 45 Hz), 6.1 (ν$_{1/2}$ = 95 Hz), 3.1 (ν$_{1/2}$ = 25 Hz), 2.8 (ν$_{1/2}$ = 25 Hz), 1.1 (ν$_{1/2}$ = 15 Hz), −2.6 (ν$_{1/2}$ = 55 Hz), −3.5 (ν$_{1/2}$ = 45 Hz), −5.1 (ν$_{1/2}$ = 50 Hz), −7.8 (ν$_{1/2}$ = 100 Hz, 9 H, NC(CH$_3$)$_3$), −23.6 (ν$_{1/2}$ = 1000 Hz), −46.4 (ν$_{1/2}$ = 100 Hz), −52.6 (ν$_{1/2}$ = 140 Hz), −73.9 (ν$_{1/2}$ = 150 Hz) ppm. **4-Gd**. Yield: Orange crystals; 216 mg (0.337 mmol, 43%). Mp.: 192 °C. Anal. calc. (%) for C$_{27}$H$_{49}$O$_2$NSiClGd (640.48 g mol^{-1}) C 50.63, H 7.71; C$_{23}$H$_{41}$ONSiClGd (loss of one coordinated THF molecule) C 48.60, H 7.27; found C 49.40, H 7.63. The low C and H values may readily be explained by partial THF loss. **4-Dy**. Yield: Yellow crystals; 192 mg (0.297 mmol, 28%). Mp.: 181 °C (rev). Anal. calc. (%) for C$_{27}$H$_{49}$SiNO$_2$ClDy (645.73 g mol^{-1}) C 50.22, H 7.65; found C 50.10, H 7.74, N 2.05. **4-Ho**. Yield: Orange crystals; 110 mg (0.170 mmol, 16%). Mp.: 182 °C (rev). Anal. calc. (%) for C$_{27}$H$_{49}$SiNO$_2$ClHo (647.75 g mol^{-1}) C 50.06, H 7.56; found C 50.09, H 7.50. **4-Er**. Yield: Orange crystals; 148 mg (0.228 mmol, 29%). Mp.: 162 °C (rev). Anal. calc. (%) for C$_{27}$H$_{49}$NO$_2$SiClEr (650.49 g mol^{-1}) C 49.85, H 7.59, N 2.15; found C 50.00, H 7.65, N 2.36. **4-Tm**. Yield: Orange crystals; 92 mg (0.141 mmol, 18%). Mp.: 176 °C. Despite several attempts, it was impossible to obtain satisfactory results from elemental analysis. This can again be attributed to the high sensitivity of this complex towards air and moisture.

General procedure for the synthesis of rare-earth metal bis(trimethylsilyl)amide complexes 7-M: The appropriate rare-earth metal chloro complex **4-M** or **5-M** (0.50 equiv., Ln = Nd; 1.00 equiv., Ln = Dy, Ho, Y) or the iodine complex **5-La** (0.50 equiv.; Ln = La) was dissolved in THF (5 mL). A solution of [Li(N(SiMe$_3$)$_2$)(OEt$_2$)]

Chemistry–A European Journal

Full Paper
doi.org/10.1002/chem.202003170

Chemistry Europe
European Chemical
Societies Publishing

Table 6. Detailed reaction times and purification methods for bis(trimethylsilyl)amide complexes.

Compound	Starting material	M [g mol⁻¹]	n [mmol]	Reaction time	Washing	Crystallisation conditions
7-Y	4-Y	572.13	0.175	1 h	n-hexane	n-hexane/THF, rt
7-La	5-La	1306.98	0.125	2 h	n-hexane	n-hexane, −30 °C
7-Nd	5-Nd	1110.73	0.0900	2.5 h	n-hexane	n-hexane, rt
7-Dy	4-Dy	645.73	0.163	12 h	n-hexane	n-hexane, rt
7-Ho	4-Ho	647.75	0.131	12 h	n-hexane	n-hexane, rt

(1.00 equiv.) in THF (3 mL) was added and the reaction mixture was stirred at ambient temperature. After completion of the reaction, the solvent was removed in vacuum and the residue was extracted with n-hexane (5 mL). After filtration through glass wool and celite, the products were crystallised and dried in vacuum. Individual information regarding the purification process of each compound can be found in Table 6. Spectroscopic data are listed below.

7-Y. Yield: Pale yellow crystals; 47 mg (0.0752 mmol, 43%). Mp.: 127 °C (rev.). Anal. calc. (%) for $C_{29}H_{59}ON_2Si_3Y$ (624.96 g mol⁻¹) C 55.73, H 9.52, N 4.48; found C 55.65, H 10.01, N 4.23. ^{1}H NMR (400 MHz, C_6D_6, 298 K): $\delta = 4.83$ (br. s, 1 H, $H5$), 4.47 (br. s, 1 H, exo-$H1$), 4.27 (s, 1 H, $H3$), 4.14 (br. s, 1 H, $endo$-$H1$), 3.80–6.69 (m, 2 H, thf(2,5)), 3.63–3.50 (m, 2 H, thf(2,5)), 2.55–2.44 (m, 2 H, $H6$), 2.44–2.34 (m, 1 H, $H8b$), 2.21 (t, 1 H, $J_{H,H} = 5.3$ Hz, $H9$), 2.15–2.05 (m, 2 H, $H7$, $H13a$), 1.84–1.76 (m, 1 H, $H13b$), 1.60 (d, 1 H, $J_{H,H} = 8.4$ Hz, $H8a$), 1.44 (s, 9 H, $NC(CH_3)_3$), 1.29 (s, 3 H, $H12$), 1.28–1.23 (m, 4 H, thf(3,4)), 1.08 (s, 3 H, $H11$), 0.45 (s, 3 H, $H14$), 0.42 (s, 18 H, $N(Si(CH_3)_3)_2$), 0.35 (s, 3 H, $H15$) ppm. $^{13}C\{^1H\}$ NMR (101 MHz, C_6D_6, 298 K): $\delta = 153.8$ (C_q), 152.4 (C_q), 95.1 (CH, $C5$), 90.5 (CH, $C3$), 88.1 (CH_2, $C1$), 71.2 (2 × CH_2, thf(2,5)), 54.1 (C_q, $NC(CH_3)_3$), 52.6 (CH, $C9$), 41.1 (CH, $C7$), 39.0 (C_q, $C10$), 34.9 (3 × CH_3, $NC(CH_3)_3$), 33.7 (CH_2, $C13$), 32.4 (CH_2, $C8$), 32.1 (CH_2, $C6$), 26.6 (CH_3, $C12$), 25.0 (2 × CH_2, thf(3,4)), 21.4 (CH_3, $C11$), 8.0 (CH_3, $C14$), 6.5 (CH_3, $C15$), 6.0 (6 × CH_3, $N(Si(CH_3)_3)_2$) ppm.

7-La. Yield: Yellow crystals; 67 mg (0.0993 mmol, 79%). Mp.: 129 °C (rev.). Anal. calc. (%) for $C_{29}H_{59}N_2OSi_3La$ (674.96 g mol⁻¹) C 51.61, H 8.81, N 4.15; found C 43.15, H 7.44, N 2.27. Despite several attempts, no better microanalytical data were obtained. However, the NMR spectra provided in the SI are within the NMR detection limits consistent with a pure product. ^{1}H NMR (400 MHz, C_6D_6, 298 K): $\delta = 5.03$ (s, 1 H, $H5$), 4.86 (s, 1 H, exo-$H1$), 4.61 (br. s, 1 H, $H3$), 4.34 (br. s, 1 H, $endo$-$H1$), 3.81 (br. s, 2 H, thf(2,5)), 3.71 (br. s, 2 H, thf(2,5)), 3.16 (d, $J_{H,H} = 15.2$ Hz, 1 H, $H6$), 2.71 (d, $J_{H,H} = 15.2$ Hz, 1 H, $H6$), 2.53–2.21 (m, 2 H, $H9$, $H8b$), 2.15 (d, $J_{H,H} = 12.1$ Hz, 2 H, $H7$, $H13a$), 2.11–2.04 (m, 1 H, $H8a$), 1.82–1.71 (m, 1 H, $H13b$), 1.58 (s, 9 H, $NC(CH_3)_3$), 1.33–1.27 (m, 7 H, thf(3,4), $H12$), 1.12 (s, 3 H, $H11$), 0.54 (s, 3 H, $H14$), 0.41 (br. s, 18 H, $N(Si(CH_3)_3)_2$), 0.25 (s, 3 H, $H15$) ppm. $^{13}C\{^1H\}$ NMR (101 MHz, C_6D_6, 298 K): $\delta = 154.2$ (C_q, $C4$), 151.4 (C_q, $C2$), 100.0 (CH, $C5$), 96.4 (CH, $C3$), 92.2 (CH_2, $C1$), 70.8 (2 × CH_2, thf(2,5)), 55.4 (C_q, $NC(CH_3)_3$), 52.5 (CH, $C9$), 41.4 (CH, $C7$), 39.1 (C_q, $C10$), 34.4 (CH_2, $C13$), 33.5 (3 × CH_3, $NC(CH_3)_3$), 32.8 (CH_2, $C6$), 32.5 (CH_2, $C8$), 26.6 (CH_3, $C12$), 25.3 (2 × CH_2, thf(3,4)), 21.4 (CH_3, $C11$), 7.8 (CH_3, $C14$), 6.9 (CH_3, $C15$), 5.0 (6 × CH_3, $N(Si(CH_3)_3)_2$) ppm. **7-Nd**. Yield: Green-red crystals (dichroic); 28 mg (0.0412 mmol, 23%). Mp.: 128 °C (rev.). Anal. calc. (%) for $C_{29}H_{59}N_2OSi_3Nd$ (680.30 g mol⁻¹) C 51.20, H 8.74, N 4.12; found C 50.40, H 7.97, N 3.67. Because of the high air- and moisture-sensitivity, no better elemental analysis was obtained for this compound. ^{1}H NMR (300 MHz, C_6D_6, 298 K): $\delta = 29.0$ ($\nu_{1/2} = 190$ Hz, 1 H), 18.0 ($\nu_{1/2} = 100$ Hz, 1 H), 8.4 ($\nu_{1/2} = 440$ Hz, 1 H), 2.6 ($\nu_{1/2} = 45$ Hz, 3 H), −0.5 ($\nu_{1/2} = 120$ Hz, 9 H), −1.3 ($\nu_{1/2} = 65$ Hz, 3 H), −2.0 ($\nu_{1/2} = 150$ Hz, 3 H), −2.9 ($\nu_{1/2} = 170$ Hz, 3 H), −4.4 (500 Hz, 9 H), −7.2 ($\nu_{1/2} = 900$ Hz, 9 H), −10.7 ($\nu_{1/2} = 300$ Hz, 2 H), −14.8 ($\nu_{1/2} = 500$ Hz, 1 H) ppm. Because of significant line broadening, not all expected resonances could be

resolved and some are overlapped. **7-Dy**. Yield: Yellow crystals; 60 mg (0.0859 mmol, 53%). Mp.: 106 °C (rev.). Anal. calc. (%) for $C_{29}H_{59}ON_2Si_3Dy$ (698.56 g mol⁻¹) C 49.86, H 8.51, N 4.01; found C 49.72, H 8.78, N 3.73. **7-Ho**. Yield: Orange crystals; 83 mg (0.118 mmol, 90%). Mp.: 130 °C (rev.). Anal. calc. (%) for $C_{29}H_{59}ON_2Si_3Ho$ (700.99 g mol⁻¹) C 49.69, H 8.48, N 4.00; found C 49.64, H 8.26, N 3.66.

General procedure for the synthesis of rare-earth metal BH₄ complexes 8-M: The appropriate rare-earth metal BH₄ complex [Ln(BH₄)₃(thf)₃] (Ln = La, Nd; 1.00 equiv.) was dissolved in THF and [K₂pdl*SiMe₂NtBu] (**3**; 1.00 equiv.), dissolved in THF, was added. The reaction mixture was stirred at ambient temperature for 12 h. After filtration of the resulting suspension, the solvent was almost completely removed under reduced pressure. The residue was then dissolved in n-hexane and a minimum amount of THF for recrystallisation at −30 °C. After removal of the supernatant liquid, the crystalline solid was washed with n-hexane and dried in vacuum.

8-La. Yield: 155 mg (0.145 mmol, 37%). Mp.: 137 °C. Anal. calc. (%) for $C_{46}H_{90}N_2O_2Si_2B_2La_2$ (1058.49 g mol⁻¹) C 52.18, H 8.57, N 2.04; $C_{42}H_{82}N_2OSi_2B_2La_2$ (loss of one coordinated THF molecule) C 51.12, H 8.38, N 2.84; found C 50.62, H 8.17, N 2.19. The complex is prone to THF loss as well as being highly air- and moisture-sensitive, which caused low values in the microanalytical data. However, the NMR spectra shown in the Supporting Information establish the purity of this compound. ^{1}H NMR (600 MHz, C_6D_6, 298 K): $\delta = 5.01$ (br. s., 1 H, $H5$), 4.70 (br. s, 1 H, exo-$H1$), 4.65–4.62 (m, 1 H, $H3$), 4.08–4.01 (m, 1 H, $endo$-$H1$), 3.96–3.86 (m, 2 H, thf(2,5)), 3.78–3.65 (m, 2 H, thf(2,5)), 3.07–3.00 (m, 2 H, $H6a$), 2.69 (d, 1 H, $J_{H,H} = 16.8$ Hz, $H6b$), 2.27–2.22 (m, 1 H, $H8b$), 2.14 (d, $J = 13.1$ Hz, 1 H, $H13a$), 2.10 (sept, $J = 2.8$ Hz, 1 H, $H7$), 2.04 (t, $J = 5.5$ Hz, 1 H, $H9$), 1.87–1.82 (m, 1 H, $H13b$), 1.57 (d, 1 H, $J_{H,H} = 8.5$ Hz, $H8a$), 1.48 (s, 9 H, $NC(CH_3)_3$), 1.37–1.31 (m, 4 H, thf(3,4)), 1.30 (s, 3 H, $H12$), 1.11 (s, 3 H, $H11$), 0.53 (s, 3 H, $H14$), 0.27 (s, 3 H, $H15$) ppm. The BH₄ resonances were overlapped by other signals and could therefore not be assigned. $^{13}C\{^1H\}$ NMR (151 MHz, C_6D_6, 298 K): $\delta = 155.1$ (C_q, $C4$), 150.9 (C_q, $C2$), 100.2 (CH, $C5$), 96.2 (CH, $C3$), 88.8 (CH_2, $C1$), 71.1 (2 × CH_2, thf(2,5)), 54.8 (C_q, $C(CH_3)_3$), 52.5 (CH, $C9$), 41.3 (CH, $C7$), 38.9 (C_q, $C10$), 34.9 (CH_2, $C13$), 33.8 (3 × CH_3, $NC(CH_3)_3$), 32.6 (CH_2, $C6$), 30.9 (CH_2, $C8$), 26.6 (CH_3, $C12$), 25.4 (2 × CH_2, thf(3,4)), 21.4 (CH_3, $C11$), 7.8 (CH_3, $C14$), 7.1 (CH_3, $C15$) ppm. $^{11}B\{^1H\}$ NMR (128 MHz, C_6D_6, 298 K): $\delta = −24.1$ ppm. FTIR (Nujol): $\tilde{\nu} = 2418$ (br, w, B-H str.), 2260 (br, w, B-H str.), 2219 (br, w, B-H str.), 1246(m), 1019 (m), 828 (w) cm⁻¹. **8-Nd**. Yield: Green-red crystals (dichroic); 62 mg (0.0580 mmol, 20%). Mp.: 126 °C. Anal. calc. (%) for $C_{46}H_{90}Si_2N_2O_2B_2Nd_2$ (1069.51 g mol⁻¹) C 51.66, H 8.48, N 2.62; found C 51.74, H 8.32, N 2.23. ^{1}H NMR (400 MHz, C_6D_6, 298 K): $\delta = 58.1$ ($\nu_{1/2} = 1800$ Hz), 47.3 ($\nu_{1/2} = 200$ Hz), 28.2 ($\nu_{1/2} = 140$ Hz), 12.9 ($\nu_{1/2} = 40$ Hz), 12.6 ($\nu_{1/2} = 120$ Hz), 10.2 ($\nu_{1/2} = 75$ Hz), 6.2 ($\nu_{1/2} = 110$ Hz), 1.9 ($\nu_{1/2} = 35$ Hz), 1.6 ($\nu_{1/2} = 140$ Hz), 0.1 ($\nu_{1/2} = 50$ Hz), −0.7 ($\nu_{1/2} = 120$ Hz), −1.0 ($\nu_{1/2} = 140$ Hz), −2.6 ($\nu_{1/2} = 600$ Hz), −4.9 ($\nu_{1/2} = 140$ Hz), −6.4 ($\nu_{1/2} = 80$ Hz), −7.3 (80 Hz), −48.2 ($\nu_{1/2} = 350$ Hz), −58.2 ($\nu_{1/2} = 310$ Hz), −73.8 ($\nu_{1/2} = 370$ Hz) ppm. $^{11}B\{^1H\}$ NMR (96 MHz, C_6D_6, 298 K): $\delta = 149.4$ ($\nu_{1/2} = 1000$ Hz) ppm. **F**TIR (Nujol):

Chemistry–A European Journal

Full Paper
doi.org/10.1002/chem.202003170

Chemistry Europe
European Chemical
Societies Publishing

$\tilde{v} = 2430$ (br, w, B-H str.), 2265 (br, m, B-H str.), 1054 (m), 1018 (m), 845 (m) cm^{-1}.

Synthesis of 9-Lu: [Lu(OTf)$_3$] (1.00 equiv.) was dissolved in THF (30 mL) inside a glovebox. A solution of [K$_2$(pdl*SiMe$_2$NtBu)] (**3**; 1.00 equiv.) was added dropwise and the reaction mixture was stirred at ambient temperature for 20 h. The solvent was removed under reduced pressure and the residue was extracted with n-hexane (60 mL). The resulting suspension was centrifuged (30 min, 3894 g, 10 °C) and the supernatant solution was filtered through glass wool and celite. After removal of the solvent, the crude product was purified by crystallisation from Et$_2$O. The crystals were washed with n-hexane and dried in vacuum. Alternatively, compound **9-Lu** could be precipitated from n-hexane to give a pale-yellow powder. Yield: 397 mg (0.284 mmol, 43 %). Mp.: 189 °C. Anal. calc. (%) for C$_{48}$H$_{82}$O$_8$N$_2$Si$_2$S$_2$F$_6$Lu$_2$ (1049.47 g mol^{-1}) C 41.20, H 5.91, N 2.00; found C 40.92, H 5.95, N 1.89. ^{1}H NMR (500 MHz, C$_6$D$_6$, 298 K): $\delta = 5.55$ (s, 1 H, $H5$), 4.54 (s, 1 H, exo-$H1$), 4.20 (s, 1 H, $endo$-$H1$), 4.10 (s, 1 H, $H3$), 4.04 (br. s, 2 H, thf(2,5)), 3.71 (br. s, 2 H, thf(2,5)), 3.13 (br. d, $J_{H,H} = 17.0$ Hz, 1 H, $H6a$), 2.70 (br. d, $J_{H,H} = 17.0$ Hz, 1 H, $H6b$), 2.32–2.24 (m, 1 H, $H8a$), 2.22 (s, 1 H, $H13a$), 2.18–2.11 (m, 1 H, $H7$), 1.97–1.90 (m, 1 H, $H9$), 1.62 (br. d, $J_{H,H} = 12.6$ Hz, 1 H, $H13b$), 1.49 (br. d, $J_{H,H} = 8.5$ Hz, 1 H, $H8b$), 1.39 (s, 9 H, NC(CH_3)$_3$), 1.33–1.25 (m, 4 H, thf(3,4)), 1.30 (s, 3 H, $H12$), 1.06 (s, 3 H, $H11$), 0.58 (s, 3 H, $H14$), 0.25 (s, 3 H, $H15$) ppm. ^{13}C{^{1}H} NMR (126 MHz, C$_6$D$_6$, 298 K): $\delta = 153.7$ (C$_q$, $C2$), 149.9 (C$_q$, $C4$), 99.9 (CH, $C5$), 89.7 (CH, $C3$), 85.4 (CH$_2$, $C1$), 72.7 (2 × CH$_2$, thf(2,5)), 53.7 (C$_q$, NC(CH$_3$)$_3$), 52.0 (CH, $C9$), 41.1 (CH, $C7$), 38.9 (C$_q$, $C10$), 34.4 (3 × CH$_3$, NC(CH$_3$)$_3$), 33.8 (CH$_2$, $C13$), 32.0 (CH$_2$, $C6$), 30.7 (CH$_2$, $C8$), 26.6 (CH$_3$, $C12$), 25.2 (2 × CH$_2$, thf(3,4)), 21.3 (CH$_3$, $C11$), 7.8 (CH$_3$, $C14$), 7.1 (CH$_3$, $C15$) ppm. ^{19}F{^{1}H} NMR (471 MHz, C$_6$D$_6$, 298 K): $\delta = -75.5$ (s, CF_3) ppm. The resonance for the CF$_3$ group was not observed in the ^{13}C{^{1}H} NMR spectrum.

General procedure for the synthesis of rare-earth metal alkyl complexes 10-Lu and 11-Lu: Complex **9-Lu** (1.00 equiv.) was dissolved in THF (5 mL) and a solution of [Mg(CH$_2$CMe$_3$)$_2$] or [Mg(CH$_2$CMe$_2$Ph)$_2$] (1.00 equiv.) in THF (5 mL) was added. The reaction mixture was stirred for 4 h at ambient temperature. The solvent was removed under reduced pressure and the residue was extracted with n-hexane (15 mL). The resulting suspension was filtered through glass wool and celite and the solution was dried. Subsequently, the product was crystallised from THF/n-hexane (R = CH$_2$CMe$_3$) or n-hexane (R = CH$_2$CMe$_2$Ph) and the crystals were washed with n-hexane and dried in vacuum. **10-Lu**. Yield: Pale yellow crystals; 29 mg (0.0466 mmol, 65 %). Mp: 115 °C. Anal. calc. (%) for C$_{28}$H$_{52}$ONSiLu (621.78 g mol^{-1}) C 54.09, H 8.43, N 2.25; found C 47.54, H 7.18, N 2.10. Despite several attempts on independently prepared and crystallised samples, consistently low C values were obtained. Nevertheless, the NMR spectra shown in the SI confirmed its purity. The unsatisfactory microanalytical data might be traced to the high sensitivity of this complex towards air and moisture during sample measurement. ^{1}H NMR (500 MHz, C$_6$D$_6$, 298 K): $\delta = 5.68$ (br. s, 1 H, $H5$), 4.16 (br. s, 1 H, $H3$), 4.15 (d, $^2J_{H,H} = 2.6$ Hz, 1 H, $endo$-$H1$), 4.07 (d, $^2J_{H,H} = 2.6$ Hz, 1 H, exo-$H1$), 3.61–3.52 (m, 2 H, thf(2,5)), 3.35 (br. s, 2 H, thf(2,5)), 2.62–2.55 (m, 1 H, $H8a$), 2.54–2.47 (m, 1 H, $H8b$), 2.15–2.09 (m, 1 H, $H13a$), 2.09–2.05 (m, 1 H, $H7$), 2.05–2.03 (m, 1 H, $H6b$), 1.91–1.86 (m, 1 H, $H13b$), 1.83–1.78 (m, 1 H, $H9$), 1.51 (s, 9 H, $H18$), 1.47 (s, 9 H, NC(CH_3)$_3$), 1.29 (s, 3 H, $H11$), 1.11 (s, 3 H, $H12$), 1.07 (br. s, 4 H, thf(3,4)), 0.77–0.73 (m, 1 H, $H6a$), 0.52 (s, 3 H, $H14$), 0.45 (d, $^2J_{H,H} = 14.5$ Hz, 1 H, $H16b$), 0.34 (d, $^2J_{H,H} = 14.5$ Hz, 1 H, $H16a$), 0.33 (s, 3 H, $H15$) ppm. ^{13}C{^{1}H} NMR (126 MHz, C$_6$D$_6$, 298 K): $\delta = 157.9$ (C$_q$, $C2$), 147.2 (C$_q$, $C4$), 100.0 (CH, $C5$), 89.7 (CH, $C3$), 83.7 (CH$_2$, $C1$), 72.1 (CH$_2$, $C16$), 71.9 (2 × CH$_2$, thf(2,5)), 54.1 (C$_q$, NC(CH$_3$)$_3$), 51.7 (CH, $C9$), 41.0 (CH, $C7$), 39.0 (C$_q$, $C10$), 37.5 (3 × CH$_3$, $C18$), 37.0 (C$_q$, $C17$), 36.1 (3 × CH$_3$, NC(CH$_3$)$_3$,

35.8 (CH$_2$, $C13$), 32.5 (CH$_2$, $C8$), 31.5 (CH$_2$, $C6$), 26.7 (CH$_3$, $C11$), 25.1 (2 × CH$_2$, thf(3,4)), 21.4 (CH$_3$, $C12$), 8.2 (CH$_3$, $C15$), 7.9 (CH$_3$, $C14$) ppm. Despite several attempts, satisfactory values for elemental analysis could not be obtained. **11-Lu**. Yield: Light yellow crystals; 26 mg (0.0380 mmol, 27 %). Mp: 125 °C. Anal. calc. (%) for C$_{33}$H$_{54}$ONSiLu (683.85 g mol^{-1}) C 57.96, H 7.96, N 2.05; found C 58.17, H 7.87, N 2.02. ^{1}H NMR (500 MHz, C$_6$D$_6$, 298 K): $\delta = 7.78$–7.74 (m, 2 H, m-C$_6$H$_5$), 7.38–7.33 (m, 2 H, o-C$_6$H$_5$), 7.13 (tt, $^4J_{H,H} = 1.2$ Hz, $^3J_{H,H} = 7.2$ Hz, 1 H, p-C$_6$H$_5$), 5.28 (s, 1 H, $H5$), 4.11 (d, $^4J_{H,H} = 2.6$ Hz, 1 H, $H3$), 3.95 (d, $^4J_{H,H} = 2.6$ Hz, 1 H, exo-$H1$), 3.77 (d, $^4J_{H,H} = 3.5$ Hz, 1 H, $endo$-$H1$), 3.55–3.45 (m, 2 H, thf(2,5)), 3.27 (br. s, 2 H, thf(2,5)), 2.55–2.48 (m, 1 H, $H6a$), 2.48–2.41 (m, 1 H, $H6b$), 2.08 (d, $^2J_{H,H} = 12.5$ Hz, 1 H, $H13a$), 2.08–2.02 (m, 2 H, $H7$, $H8b$), 1.85 (dd, $^4J_{H,H} = 3.5$ Hz, $^2J_{H,H} = 12.5$ Hz, 1 H, $H13b$), 1.82 (s, 3 H, $H18$), 1.79 (s, 3 H, $H18$), 1.78–1.75 (m, 1 H, $H9$), 1.38 (s, 9 H, NC(CH_3)$_3$), 1.28 (s, 3 H, $H12$), 1.06 (s, 7 H, $H11$, thf(3,4)), 0.76 (d, $^2J_{H,H} = 12.4$ Hz, 1 H, $H16b$), 0.71 (d, $J_{H,H} = 6.9$ Hz, 1 H, $H8a$), 0.59 (d, $^2J_{H,H} = 12.4$ Hz, 1 H, $H16a$), 0.53 (s, 3 H, $H14$), 0.32 (s, 3 H, $H15$) ppm. ^{13}C{^{1}H} NMR (126 MHz, C$_6$D$_6$, 298 K): $\delta = 158.0$ (C$_q$, $C2$), 157.2 (C$_q$, i-C$_6$H$_5$), 147.2 (C$_q$, $C4$), 128.4 (2 × CH, o-C$_6$H$_5$), 125.8 (2 × CH, m-C$_6$H$_5$), 124.7 (CH, p-C$_6$H$_5$), 99.9 (CH, $C5$), 89.7 (CH, $C3$), 84.1 (CH$_2$, $C1$), 72.4 (CH$_2$, $C16$), 71.9 (2 × CH$_2$, thf(2,5)), 54.0 (C$_q$, NC(CH$_3$)$_3$), 51.7 (CH, $C9$), 43.2 (C$_q$, $C17$), 41.0 (CH, $C7$), 39.0 (C$_q$, $C10$), 36.7 (CH$_3$, $C18$), 36.1 (CH$_3$, $C18$), 35.9 (3 × CH$_3$, NC(CH$_3$)$_3$), 35.7 (CH$_2$, $C13$), 32.7 (CH$_2$, $C6$), 31.4 (CH$_2$, $C8$), 26.7 (CH$_3$, $C12$), 25.1 (2 × CH$_2$, thf(3,4)), 21.4 (CH$_3$, $C11$), 8.0 (CH$_3$, $C15$), 7.9 (CH$_3$, $C14$) ppm.

Conflict of interest

The authors declare no conflict of interest.

[1] W. E. Piers, P. J. Shapiro, E. E. Bunel, J. E. Bercaw, *Synlett* **1990**, 74 – 84.
[2] a) J. Okuda, *Dalton Trans.* **2003**, 2367 – 2378; b) J. Cano, K. Kunz, *J. Organomet. Chem.* **2007**, *692*, 4411 – 4423.
[3] a) J. E. Bercaw, *Pure Appl. Chem.* **1990**, *62*, 1151 – 1154; b) P. J. Shapiro, E. Bunel, W. P. Schaefer, J. E. Bercaw, *Organometallics* **1990**, *9*, 867 – 869; c) P. J. Shapiro, W. P. Schaefer, J. A. Labinger, J. E. Bercaw, W. D. Cotter, *J. Am. Chem. Soc.* **1994**, *116*, 4623 – 4640.
[4] J. Okuda, *Chem. Ber.* **1990**, *123*, 1649 – 1651.
[5] R. D. Ernst, *Chem. Rev.* **1988**, *88*, 1255 – 1291.
[6] a) S. A. Solomon, F. M. Bickelhaupt, R. A. Layfield, M. Nilsson, J. Poater, M. Solà, *Chem. Commun.* **2011**, *47*, 6162 – 6164; b) B. M. Day, J. J. W. McDouall, J. Clayden, R. A. Layfield, *Organometallics* **2015**, *34*, 2348 – 2355.
[7] B. M. Day, N. F. Chilton, R. A. Layfield, *Dalton Trans.* **2015**, *44*, 7109 – 7113.
[8] A. C. Fecker, B.-F. Crǎciun, P. Schweyen, M. Freytag, P. G. Jones, M. D. Walter, *Organometallics* **2015**, *34*, 146 – 158.
[9] a) V. M. Arredondo, S. Tian, F. E. McDonald, T. J. Marks, *J. Am. Chem. Soc.* **1999**, *121*, 3633 – 3639; b) F. Pohlki, I. Bytschkov, H. Siebeneicher, A. Heutling, W. A. König, S. Doye, *Eur. J. Org. Chem.* **2004**, 1967 – 1972.
[10] a) A. C. Fecker, A. Glöckner, C. G. Daniliuc, M. Freytag, P. G. Jones, M. D. Walter, *Organometallics* **2013**, *32*, 874 – 884; b) A. C. Fecker, B.-F. Crǎciun, M. Freytag, P. G. Jones, M. D. Walter, *Organometallics* **2014**, *33*, 3792 –

3803; c) A. C. Fecker, M. Freytag, P. G. Jones, N. Zhao, G. Zi, M. D. Walter, *Dalton Trans.* **2015**, *44*, 16325–16331; d) A. C. Fecker, K. Münster, M. Freytag, P. G. Jones, M. D. Walter, *Eur. J. Inorg. Chem.* **2019**, 3954–3961; e) A. C. Fecker, M. Freytag, P. G. Jones, M. D. Walter, *Dalton Trans.* **2019**, *48*, 8297–8302.

[11] R. D. Shannon, *Acta Crystallogr. Sect. A* **1976**, *32*, 751–767.

[12] J. Raeder, M. Reiners, R. Baumgarten, K. Münster, D. Baabe, M. Freytag, P. G. Jones, M. D. Walter, *Dalton Trans.* **2018**, *47*, 14468–14482.

[13] a) M. Reiners, A. C. Fecker, M. Freytag, P. G. Jones, M. D. Walter, *Dalton Trans.* **2014**, *43*, 6614–6617; b) B. M. Day, J. Clayden, R. A. Layfield, *Organometallics* **2013**, *32*, 4448–4451; c) H. Yasuda, M. Yamauchi, A. Nakamura, T. Sei, Y. Kai, N. Yasuoka, N. Kasai, *Bull. Chem. Soc. Jpn.* **1980**, *53*, 1089–1100.

[14] M. R. Kunze, D. Steinborn, K. Merzweiler, C. Wagner, J. Sieler, R. Taube, *Z. Anorg. Allg. Chem.* **2007**, *633*, 1451–1463.

[15] a) M. P. Conley, G. Lapadula, K. Sanders, D. Gajan, A. Lesage, I. del Rosal, L. Maron, W. W. Lukens, C. Copéret, R. A. Andersen, *J. Am. Chem. Soc.* **2016**, *138*, 3831–3843; b) Z. Dawoodi, M. L. H. Green, V. S. B. Mtetwa, K. Prout, *Chem. Commun.* **1982**, 802–803; c) Z. Dawoodi, M. L. H. Green, V. S. B. Mtetwa, K. Prout, A. J. Schultz, J. M. Williams, T. F. Koetzle, *Dalton Trans.* **1986**, 1629–1637; d) A. G. Avent, C. F. Caro, P. B. Hitchcock, M. F. Lappert, Z. Li, X.-H. Wei, *Dalton Trans.* **2004**, 1567–1577; e) P. B. Hitchcock, M. F. Lappert, R. G. Smith, R. A. Bartlett, P. P. Power, *Chem. Commun.* **1988**, 1007–1009; f) N. Koga, K. Morokuma, *J. Am. Chem. Soc.* **1988**, *110*, 108–112.

[16] T. D. Tilley, R. A. Andersen, A. Zalkin, *Inorg. Chem.* **1984**, *23*, 2271–2276.

[17] a) M. Visseaux, F. Bonnet, *Coord. Chem. Rev.* **2011**, *255*, 374–420; b) F. Bonnet, C. E. Jones, S. Semlali, M. Bria, P. Roussel, M. Visseaux, P. L. Arnold, *Dalton Trans.* **2013**, *42*, 790–801; c) S. Fadlallah, J. Jothieswaran, F. Capet, F. Bonnet, M. Visseaux, *Chem. Eur. J.* **2017**, *23*, 15644–15654; d) S. Fadlallah, M. Terrier, C. Jones, P. Roussel, F. Bonnet, M. Visseaux, *Organometallics* **2016**, *35*, 456–461; e) J. Kratsch, M. Kuzdrowska, M. Schmid, N. Kazeminejad, C. Kaub, P. Oña-Burgos, S. M. Guillaume, P. W. Roesky, *Organometallics* **2013**, *32*, 1230–1238; f) T. P. Seifert, T. S. Brunner, T. S. Fischer, C. Barner-Kowollik, P. W. Roesky, *Organometallics* **2018**, *37*, 4481–4487; g) J. Liu, L. Nodaraki, P. Cobb, M. Giansiracusa, F. Ortu, F. Tuna, D. P. Mills, *Dalton Trans.* **2020**, *49*, 6504–6511.

[18] M. Visseaux, M. Terrier, A. Mortreux, P. Roussel, *Eur. J. Inorg. Chem.* **2010**, 2867–2876.

[19] a) S. M. Cendrowski-Guillaume, M. Nierlich, M. Lance, M. Ephritikhine, *Organometallics* **1998**, *17*, 786–788; b) F. Jaroschik, F. Bonnet, X.-F. Le Goff, L. Ricard, F. Nief, M. Visseaux, *Dalton Trans.* **2010**, *39*, 6761–6766.

[20] G. G. Skvortsov, M. V. Yakovenko, P. M. Castro, G. K. Fukin, A. V. Cherkasov, J.-F. Carpentier, A. A. Trifonov, *Eur. J. Inorg. Chem.* **2007**, 3260–3267.

[21] D. Barbier-Baudry, O. Blacque, A. Hafid, A. Nyassi, H. Sitzmann, M. Visseaux, *Eur. J. Inorg. Chem.* **2000**, 2333–2336.

[22] F. Ortu, D. Packer, J. Liu, M. Burton, A. Formanuik, D. P. Mills, *J. Organomet. Chem.* **2018**, *857*, 45–51.

[23] a) J. Jenter, G. Eickerling, P. W. Roesky, *J. Organomet. Chem.* **2010**, *695*, 2756–2760; b) N. Meyer, J. Jenter, P. W. Roesky, G. Eickerling, W. Scherer, *Chem. Commun.* **2009**, 4693–4695.

[24] T. J. Marks, J. R. Kolb, *Chem. Rev.* **1977**, *77*, 263–293.

[25] a) M. Nishiura, F. Guo, Z. Hou, *Acc. Chem. Res.* **2015**, *48*, 2209–2220; b) P. L. Watson, G. W. Parshall, *Acc. Chem. Res.* **1985**, *18*, 51–56.

[26] a) D. Barisic, D. A. Buschmann, D. Schneider, C. Maichle-Mössmer, R. Anwander, *Chem. Eur. J.* **2019**, *25*, 4821–4832; b) C. O. Hollfelder, L. N. Jende, H.-M. Dietrich, K. Eichele, C. Maichle-Mössmer, R. Anwander, *Chem. Eur. J.* **2019**, *25*, 7298–7302; c) M. R. Kunze, R. Taube, *Z. Anorg. Allg. Chem.* **2010**, *636*, 2454–2461.

[27] a) K. R. D. Johnson, P. G. Hayes, *Chem. Soc. Rev.* **2013**, *42*, 1947–1960; b) G. Song, W. N. O. Wylie, Z. Hou, *J. Am. Chem. Soc.* **2014**, *136*, 12209–12212.

[28] a) N. Kazeminejad, D. Munzel, M. T. Gamer, P. W. Roesky, *Chem. Commun.* **2017**, *53*, 1060–1063; b) G. Luo, F. Liu, Y. Luo, G. Zhou, X. Kang, Z. Hou, L. Luo, *Organometallics* **2019**, *38*, 1887–1896.

[29] a) Y. Luo, W. Li, D. Lin, Y. Yao, Y. Zhang, Q. Shen, *Organometallics* **2010**, *29*, 3507–3514; b) H. Schumann, J. A. Meese-Marktscheffel, A. Dietrich, J. Pickardt, *J. Organomet. Chem.* **1992**, *433*, 241–252; c) Y. Yang, B. Liu, K. Lv, W. Gao, D. Cui, X. Chen, X. Jing, *Organometallics* **2007**, *26*, 4575–4584.

[30] T. P. Gompa, N. T. Rice, D. R. Russo, L. M. Aguirre Quintana, B. J. Yik, J. Bacsa, H. S. La Pierre, *Dalton Trans.* **2019**, *48*, 8030–8033.

[31] R. A. Andersen, G. Wilkinson, *Dalton Trans.* **1977**, 809–811.

[32] H. W. Bosch, H. U. Hund, D. Nietlispach, A. Salzer, *Organometallics* **1992**, *11*, 2087–2098.

[33] U. Wannagat, G. Schreiner, *Monatsh. Chem.* **1965**, *96*, 1889–1894.

[34] a) T. J. Woodman, M. Schormann, D. L. Hughes, M. Bochmann, *Organometallics* **2004**, *23*, 2972–2979; b) D. Barisic, D. Schneider, C. Maichle-Mössmer, R. Anwander, *Angew. Chem. Int. Ed.* **2019**, *58*, 1515–1518; *Angew. Chem.* **2019**, *131*, 1528–1532.

[35] a) G. M. Sheldrick, *SHELX*, Göttingen, **1997**; b) G. M. Sheldrick, *Acta Crystallogr. Sect. A* **2008**, *64*, 112–122.

[36] E. Kováts, *Helv. Chim. Acta* **1958**, *41*, 1915–1932.

[37] Several crystallisation conditions were explored: Only amorphous material was obtained from n-hexane solutions, but in the case of diethyl ether a few crystals of **4-Y*** and **4-Tm*** were isolated, which can be attributed to a small Li$^+$ ion contamination originating from the deprotonation of **2** using the Schlosser base (Scheme 1). This results in a different structural motif, in which two ligands coordinate to the metal ion in an η^3-/κ-*N*- and κ-C1/κ-*N*-mode, respectively. Furthermore, the lithium atom is coordinated in η^5-mode by the second pdl unit along with two diethyl ether molecules. The small yield, in which **4-Y*** and **4-Tm*** were obtained, prevented further characterisation of these materials, but their structural data are available in the Supporting Information.